Clim. Past, 10, 1673–1692, 2014
www.clim-past.net/10/1673/2014/
doi:10.5194/cp-10-1673-2014

Climate of the Past
Open Access

Sediment sequence and site formation processes at the Arbreda Cave, NE Iberian Peninsula, and implications on human occupation and climate change during the Last Glacial

M. Kehl[1], E. Eckmeier[2,3], S. O. Franz[4], F. Lehmkuhl[3], J. Soler[5], N. Soler[5], K. Reicherter[6], and G.-C. Weniger[7]

[1]Institute of Geography, University of Cologne, Otto-Fischer-Str. 4, 50674 Cologne, Germany
[2]INRES-Soil Science, University of Bonn, Nussallee 13, 53115 Bonn, Germany
[3]Department of Geography, Physical Geography and Geoecology, RWTH Aachen University, Wüllnerstraße 5b, 52056 Aachen, Germany
[4]Steinmann Institute for Geology, Mineralogy and Palaeontology, University of Bonn, Nussallee 8, 53115 Bonn, Germany
[5]Universitat de Girona, Facultat de Lletres, Plaç a Ferrater i Mora 1, 17071 Girona, Spain
[6]Institute of Neotectonics & Natural Hazards, RWTH Aachen University, Lochnerstraße 4–20, 52056 Aachen, Germany
[7]Neanderthal Museum, Talstr. 300, 40822 Mettmann, Germany

Correspondence to: M. Kehl (kehlm@uni-koeln.de)

Received: 27 January 2014 – Published in Clim. Past Discuss.: 13 March 2014
Revised: 9 July 2014 – Accepted: 6 August 2014 – Published: 9 September 2014

Abstract. The Arbreda Cave provides a detailed archaeological record of the Middle to Upper Palaeolithic and is a key site for studying human occupation and cultural transitions in NE Iberia. Recently, studies of lake archives and archaeological sites presented new evidence on climate changes in NE Iberia correlating with Heinrich events. It, therefore, needs to be determined whether climate signals can be identified in the cave sequence of Arbreda, and if so, whether these signals can be correlated with stratigraphic indicators suggesting the continuity or discontinuity of human occupation.

We conducted a high-resolution sedimentological and geochemical study, including micromorphological investigations, to shed light on stratigraphy, processes of sediment accumulation and post-depositional alteration in the cave.

Seven major sediment units were distinguished which partly correlate with archaeological levels. The lower part of the sequence including Mousterian levels J and K consists of fluvial deposits truncated by a sharp erosional disconformity between Mousterian levels J and I. Strong enrichment with phosphorus and strontium reflect zoogenic inputs. The transition from Mousterian to Archaic Aurignacian in levels I and H, respectively, is reflected by more gradual changes in colour, grain size and geochemical composition. However, a peak in potentially wind-blown particles (40–125 µm in diameter) reflects higher aeolian input, and banded microstructure suggests reworking of sediments at the interface. Both properties correlate with low density of finds suggesting low intensity of human occupation related to a dry spell. More arid conditions than during the Holocene are indicated for the Gravettian to Solutrean levels. These findings are in agreement with previous palaeoclimatic interpretations as based on palaeontological proxies.

The detailed multi-proxy analyses of the sequence adds to our understanding on sediment accumulation and alteration in the Arbreda Cave. The transition from the Middle to Upper Palaeolithic probably includes a gap in human occupation. Assessing the significance and duration of this gap and correlating the climate signal requires three-dimensional reconstructions of find densities and more reliable geochronological control.

1 Introduction

Northeastern Iberia has a long and detailed archaeological record starting in the Middle Pleistocene and covering all major archaeological phases of the Middle to Upper Palaeolithics (e.g. D'Errico and Sánchez-Goñi, 2003; Saladié

et al., 2008; Martínez et al., 2010). The region has played an important role concerning the arrival of anatomically modern humans in the Iberian Peninsula (IP; e.g. Maroto et al., 1996; Zilhão, 2006; Soler et al., 2008), who, coming from the Northeast, may have met the Neanderthals at around 40 ka. However, the low reliability of radiocarbon dates of this age obscures chronometric evidence for a possible coexistence (e.g. Maroto et al., 2005; Zilhao, 2006; Maroto et al., 2012; Schmidt et al., 2012; Wood et al., 2013). Through reviewing the lithology and stratigraphy of cave sequences in the IP, Mallol et al. (2012) found sediment unconformities and/or archaeologically sterile layers between Middle and Upper Palaeolithic layers in most sites indicating that sediment accumulation was not continuous but interrupted by hiatuses of unknown duration. These hiatuses strongly suggest discontinuous occupation of the cave sites, as documented for Cova Gran (Martínez-Moreno et al., 2010). This together with variations in settlement patterns of hunter–gatherer populations in the IP may have been related to rapid climate changes (D'Errico and Sánchez-Goñi, 2003; Sepulchre et al., 2007; Bradtmöller et al., 2010; Schmidt et al., 2012). In addition, Aubry et al. (2011) assumed that climate change might have triggered partial erosion of archaeological sequences.

Variations in climate during the last glacial period in the IP is documented in diverse proxy data from terrestrial and marine archives such as pollen, geochemical signatures or sediment structures (for excellent reviews see Gonzalez-Sampériz et al., 2010; Moreno et al., 2012). The data suggest humid and cold conditions during Marine Isotope Stage (MIS) 4, a highly variable MIS 3 with abrupt and short climatic changes, and a dry and cold MIS 2 with steppe character. Burjachs and Allué (2003) presented a synthetic pollen diagram for the last glacial period of NE Iberia in which changing proportions in arboreal pollen, *Pinus*, Poaceae and *Artemisia* clearly reflect changes from warm to cool and from moist to dry conditions. At Abric Romaní (Burjachs et al., 2012), the pollen record shows a good correlation to Dansgaard–Oeschger cycles with low percentages in Pinus and arboreal pollen and concomitant increases in Asteraceae, *Artemisia* and Poaceae during stadials. For the interval from 50 to 47 ka, expansion of mixed steppes and cold and arid climate conditions were deduced, and these were correlated with Heinrich Event (H) 5 (see Burjachs et al., 2012). H 5 was followed by a change to more humid and warm climatic conditions during Greenland Interstadial 12 which, as based on micro-mammal assemblages at Abric Romaní (López-García and Cuenca-Bescós, 2010), was probably cooler and moister than today. The major shift from precipitation of travertine in archaeological level B to aeolian deposition of silts in archaeological level A in Abric Romaní was related to aridization caused by H 4 (Courty and Vallverdu, 2001). Changes in pollen composition during MIS 2 at Lake Banyoles (Pérez-Obiol and Julià, 1994; Burjachs and Allué, 2003) suggest further short-term vegetation changes triggered by climatic fluctuations including an interstadial event between 30 and 27 ka. Recently, Höbig et al. (2012) deduced climatic fluctuations by identifying several major peaks in potassium/calcium ratios in a sediment core from Lake Banyoles. Although age models based on either U-series or radiocarbon dating were not consistent and the correlation of geochemical ratios with dry or humid intervals with stadials and interstadials remains uncertain, it appears likely that some of these peaks correlate with H 5 and 4 as well as H 2–0. Finally, Daura et al. (2013) presented new palaeontological evidence and radiocarbon data indicating that during Heinrich Stadial 4 cold and dry climatic conditions and Eurasian steppe-tundra occurred in the coastal area immediately south of the city of Barcelona. Given the abovementioned evidence, it is very likely that Heinrich events or stadials were the driest and coolest periods in NE Iberia, which may also be true for other parts of the IP (see Höbig et al., 2012; Schmidt et al., 2012; López-García et al., 2013).

Lake Banyoles is located about 4 km south of Arbreda Cave, which is a key site for studying cultural change in NE Iberia, because its sequence records all major cultural techno-complexes from the late Middle Palaeolithic to the Solutrean. Theoretically, it is possible that the rapid climate and environmental changes during MIS 3 and MIS 2 in NE Iberia have affected natural processes of sediment accumulation, mixing and weathering at Arbreda. For example, changes towards colder and drier climatic conditions might have triggered or intensified frost slabbing, aeolian influx and colluvial inputs by low-energy sheet flow. However, considering the often coarse-grained stratigraphy of cave sequences, events of rapid climate change could not be recorded.

Here, we revisit the sedimentary sequence at Arbreda Cave reviewing previous work on the stratigraphic sequence and palaeontological indicators of environmental change. Furthermore, we present results of a high-resolution study on sediment colour, granulometry, geochemistry and micromorphology of the north profile in square E_0. The aims of this study are to identify changes in sediment origin and post-depositional alteration, as well as possible interruptions in the stratigraphic record resulting from climate change or depositional hiatuses. Finally, we discuss a possible gap in occupation during the transition from the Middle to the Upper Palaeolithic. These findings are synthesized in order to improve our understanding of sediment accumulation and alteration processes, as well as the role of climate and occupation history at this key site in NE Iberia.

2 Geographical setting and stratigraphic sequence

The Arbreda Cave is located at 42°09′34″ N and 2°44′45″ E at an altitude of 206 m and about 9 m above the modern valley floor of the Serinyadell River, a small creek, which drains the valley towards the north (Fig. 1). The river accumulated a fluvial terrace, about 10 m wide, which is episodically flooded

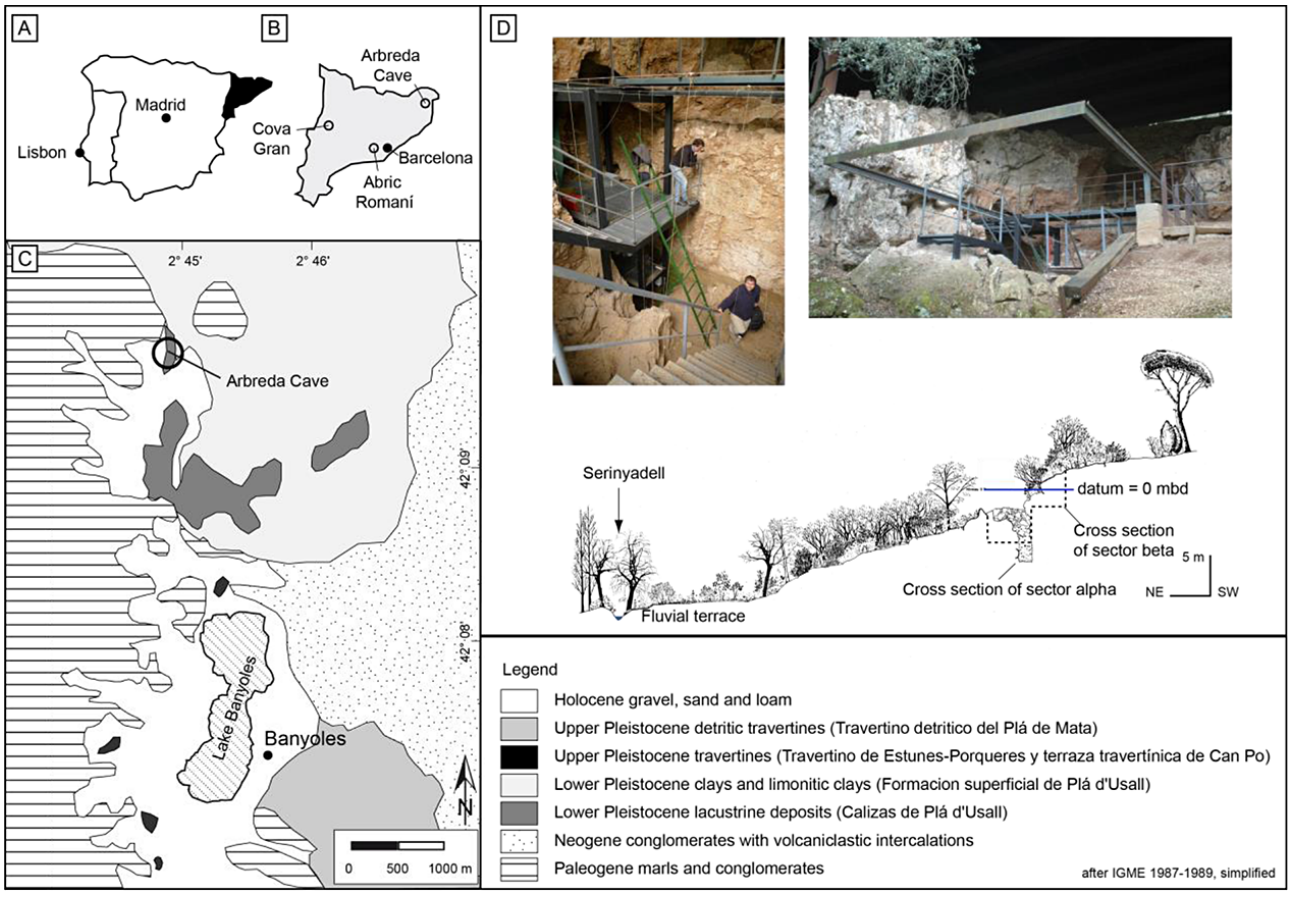

Figure 1. Location of l'Arbreda Cave on the Iberian Peninsula **(A, B)**, simplified geological map **(C)** after IGME (1987–1989), photographs of the cave and cross section (after Soler and Maroto, 1987a, changed) through the eastern part of the valley of the Serinyadell River **(D)**. Note the small altitudinal difference between the river and the lowest sediment fill of the excavation in sector alpha.

during extreme runoff events. The sediment sequence of Arbreda Cave is filling a partly collapsed cavity within the western fringe of the travertine terrace of Usall (Julià, 1980; IGME, 1987–1989), where other well-known caves including Reclau Viver, Mollet I and Pau are located in close vicinity (Soler, 1999). The original dimensions and exact morphology of the site are presently uncertain because it has not been completely excavated and its roof is almost totally collapsed. The dating of the main travertine structures still in place has yielded results between 190 and 250 ka ago, which may frame the period in which the Arbreda Cave was built by waterfalls flowing from the Usall platform.

Before archaeological excavations began, the Arbreda Cave was only a small hollow within a travertine block. In 1972, Josep Maria Corominas started a sondage into the hollow and also in front of it. Outside the hollow, he was able to excavate a 9 m deep test pit (alpha sector, Fig. 2a). This sondage revealed a long prehistoric stratigraphy, which included Neolithic, Upper Palaeolithic and Middle Palaeolithic levels. In 1975, a new research team including a member of our group (N. Soler) started to excavate and enlarge the Corominas sondage using a modern methodology (beta sector). Since then several Solutrean, Gravettian, Aurignacian and Mousterian levels have been excavated.

Soler and Maroto (1987a) reviewed previous descriptions of the stratigraphic sequence for sectors alpha, beta and gamma. They propose the following subdivision: Holocene deposits of unit A (which was also called the *terra rossa unit*) reaching down to about 2 m below datum (mbd); and Pleistocene deposits consisting of an upper sequence (unit B.1, *seqüència superior*, lower boundary at 6.3 mbd) and a lower one (unit B.2, *seqüència inferior*). The lower sequence was subdivided into units B2.1 and B2.2 with lower boundaries of 7.5 mbd and 8.8 mbd, respectively.

Soler and Maroto (1987a) describe unit A as being composed of reddish brown ferruginous loam with a polygonal secondary structure, many travertine stones and boulders up to more than 1 m in length, and occasional stones of other petrographic composition (mainly sandstone). Snail shells of terrestrial molluscs and bone fragments of micro-mammals are abundant. The unit does not show a distinct archaeological level, but locally contains ceramics of the Neolithic,

Bronze or Roman ages besides human bone and other archaeological materials. The lower boundary of unit A is sharp.

Sediment unit B.1 consists of lighter coloured clay loams with variable admixtures of sand. In the upper part, it is rich in travertine blocks and stones as well as stalagmite fragments, some covered by concretions of secondary carbonate. Unit B.1 includes nine Palaeolithic levels (Soler and Maroto, 1987b) starting with level A at the top, which contains scattered finds of indeterminate post-Solutrean affinity (see also cultural sequence of square E_0 in Fig. 2c). Level B is a poor archaeological assemblage of the Upper Solutrean with findings of abrupt notched points of Mediterranean type. The sediment properties are nearly the same as in level A. The following level C has a slightly darker colour due to burned residues, and it contains fragments of stalagmites and travertine as well as archaeological objects covered by secondary carbonate. This Solutrean level is the first rich archaeological assemblage and contains abundant faunal remains. The next level (D) represents a less rich assemblage in an almost identical sedimentary context, which was re-assigned to the Gravettian due to new dating evidence. In between 3.4 and 4.6 mbd, large travertine blocks are found indicating a major collapse of the cave roof. Below this layer, the concentration and size of blocks is decreasing downwards, but there are significant lateral differences in coarse particle contents. The finds of archaeological levels E, a rich Gravettian assemblage, and F, a more dispersed and comparatively poor Gravettian assemblage, are embedded between the boulders of the major roof fall. The dark colour of level E is related to frequent abundances of charcoal and ash. Underneath the boulder-rich layer, in the lower part of the upper sequence, more homogeneous clay loams with occasional distinctly weathered stones are present. At the top of these sediments, the archaeological level G yielded the richest assemblage belonging to Evolved Aurignacian. Below this level, archaeological finds of Archaic Aurignacian (level H) were discovered. This level is granulometrically variable with very few stones and clayey matrix in sector alpha, and a high stone content with rather sandy matrix in sector beta. Apparently, in both sectors, the sediments of level H rest conformably on the slightly darker coloured sediments of level I. This level contains the uppermost Middle Palaeolithic material and is rich in lithics. Of special interest are three Châtelperronian points found at its top which indicate that level I corresponds to a Late Mousterian.

In comparison to Upper Palaeolithic levels, which are spatially limited, the Late Mousterian level I spreads all along the excavation area and is much thicker. We interpret its large thickness as the result of a long accumulation period confirmed by the clear internal evolution of its archaeological materials. This evolution shows a trend towards more anthropogenic accumulations of faunal remains towards the end of the Mousterian. The basis of level I, for example, lacks the representative amounts of horses, bovines, reindeers and caprines found on the top of it (Maroto, 1994). Moreover, fading of charcoal remains towards the basis reinforces the idea of minor human use of the surrounding resources during the beginning of level I. However, abundant lithic artifacts all along level I and the finding of bones with cut marks and fire marks at the bottom indicate that humans considerably contributed to accumulation of level I. The most prominent faunal remains within level I are from *Ursus spelaeus* (Soler et al., 2012), which indicates that human occupations of the site, although recurrent, will have been short.

Level I has a very sharp lower boundary at about 6.3 mbd. The sediments unconformably rest on the yellowish sandy loams to silty sands of the lower sequence (*seqüència inferior*). Its upper part, unit B.2.1, consists of bright reddish loam with very low stone content, and a complete lack of boulders. The most striking features are yellow patches of phosphate. The lower part, unit B.2.2, is slightly darker coloured but still patchy and concretions of manganese are frequent in the lowest strata, which overly the bedrock. Few heavily weathered boulders and stones are present and below about 8 mbd, the coarse fraction disappears. The sediments of the lower sequence are described as being strongly altered (Soler and Maroto, 1987a). The lower sequence contains Mousterian level J, which is comparatively poor in lithics and faunal remains, as well as Mousterian levels K–N, of which levels L, M and N are very rich in lithics and faunal remains.

3 Previous studies

Kabiri (1993) conducted a comprehensive mineralogical and geochemical study on the north profile of sector alpha. The uppermost unit V of Kabiri (1993) corresponds with unit A of Soler and Maroto (1987a), whereas units IV, II, IIb and IIa correlate with unit B.1 and I with B.2.1. Unit B.2.2 of Soler and Maroto (1987a) was not sampled. Data on the magnetic susceptibility of the Arbreda sequence are presented by Ellwood et al. (2001), who used cyclic changes in susceptibility values with depth as indicators of palaeoclimatic changes and for stratigraphic purposes. The results of Kabiri (1993) and Ellwood et al. (2001) are discussed below. Some additional sedimentological data for levels I and J are presented by Bischoff et al. (1989).

The pollen content of Arbreda Cave was studied by several authors (e.g. Geurts, 1979; Loublier, 1978; Burjachs, 1987). Burjachs and Renault-Miskovsky (1992) review the previous palynological investigations and discuss pollen analysis on 53 sediment samples taken from a column of square E_0 in sector alpha (Fig. 2a). Overall, 11 pollen zones representing vegetation types from Pleistocene steppes to meso-thermophilous Holocene woodland are identified. Palaeoclimatic conditions are interpreted to have changed between cold and dry, e.g. during the final Mousterian (level I) to warm and humid during the Holocene. Burjachs and Miskovsky (1992) conclude that the pollen results are in good agreement with species assemblages

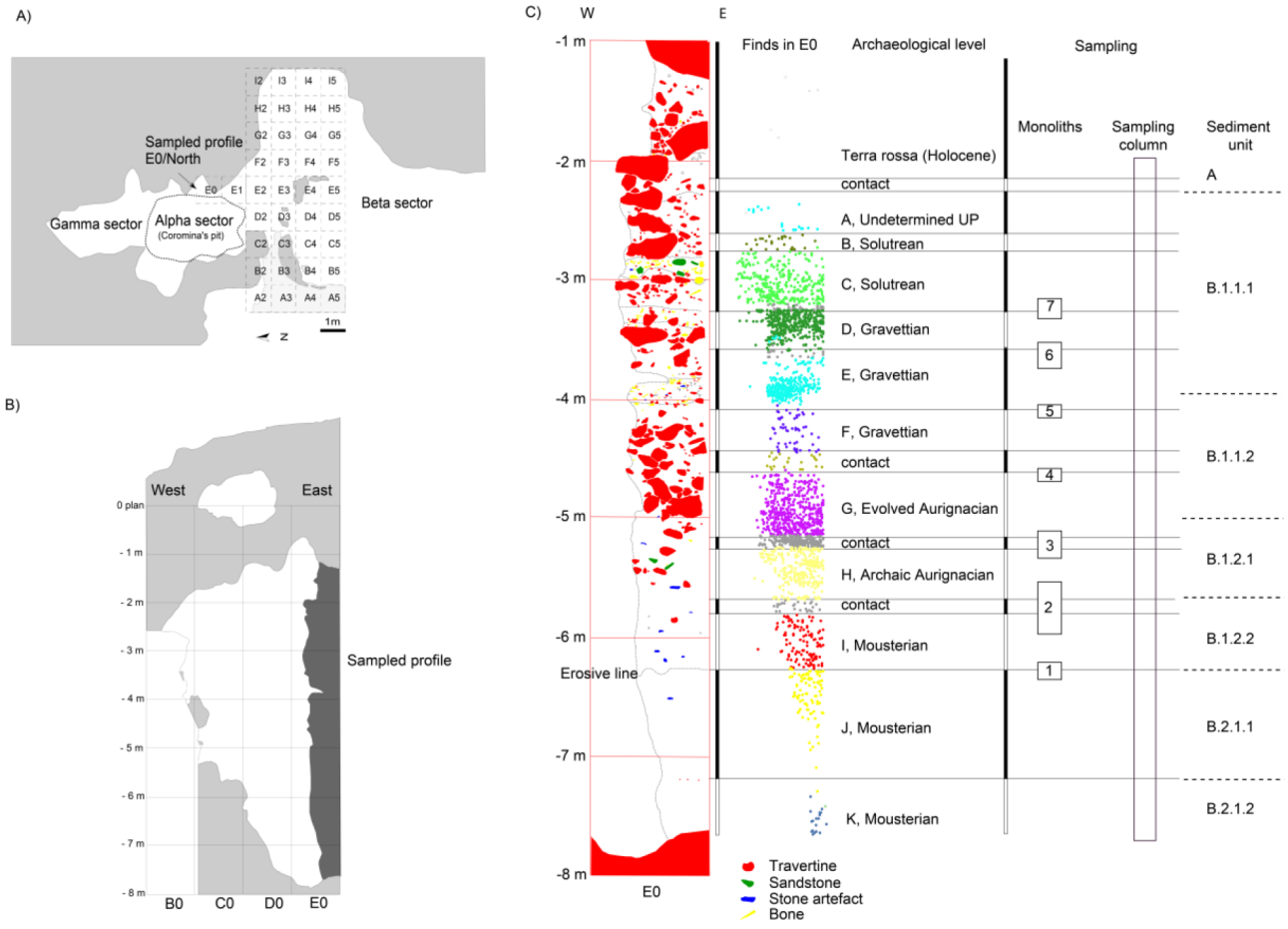

Figure 2. Excavation plan **(A)** and the north profile at square E_0 **(B)** with projected locations of archaeological finds from square E_0, and cultural attribution of these finds **(C)**. Profile sampling was conducted along a c. 20 cm wide column in the north profile, except of archaeological levels E and D, which were sampled at the east profile of square E_0. Monoliths for preparation of thin sections were taken from suspected or obvious transitions between selected archaeological levels. Boundaries between sediment units were delineated by field evidence, except for the lower boundary of unit B.1.1.1 which was geochemically defined by a sudden rise in phosphorus, copper and zinc.

and palaeoclimatic reconstructions derived from anthracological analysis (Ros, 1987) and micro-mammals (Alcalde, 1987). Besides temperature changes, the micro-mammal assemblages testify several changes between open and more forested landscapes during the Pleistocene.

Faunistic studies of large mammals (e.g. Casellas and Maroto, 1986; Estévez, 1979, 1987; Soler and Maroto, 1987b; Maroto, 1994) indicate a diversified landscape during the evolved Aurignacian (level G) with identical percentages of deer, horse and bovids. Within Gravettian levels F and E, horse becomes the dominant species. A shift toward colder temperatures during the uppermost Gravettian (level D) and Solutrean level C is indicated by a find of *Ovibos moschatus*, while horse is still dominant. Estévez (1979) also analyse the lower part of the cave sequence. Horse, deer and bovids are the dominant herbivores in levels H and I. Among the carnivores, a low number of finds are recorded for *Canis lupus*, *Vulpes vulpes*, *Crocuta spelaea* and *Lynx spelaea*, whereas *Ursus spelaeus* is represented by numerous finds in archaeological level I and below (Soler et al., 2012).

4 Materials and methods

The sequence of Arbreda Cave was studied at the north profile of square E_0 (Fig. 2b and c). This profile is a remnant of the excavation of Corominas and covers the lowermost part of unit A and the complete sequence of units B.1 and B.2.1 according to Soler and Maroto (1987a). In comparison to other profiles located along N–S and E–W transects of the beta sector, the studied profile shows a high content of fines and less boulders, allowing for high-resolution sampling of the transition from the Middle to Upper Palaeolithic.

In the field, six sediment units were distinguished from top to the bottom. These units mostly correlate with those reported by Soler and Maroto (1987a) but lower boundaries slightly differ and the distinction made in this paper is more

detailed. However, we used the same numbering system and added subunits where needed (Fig. 2). Unit B.1, the upper sequence (*seqüència superior*), was subdivided in the field into an upper part (unit B.1.1) that was very rich in travertine stones and boulders and extends down to about 5 mbd, and a lower part (unit B.1.2) which consisted of silty loams with very few limestone fragments or weathered sandstone gravel. In its upper part (B.1.2.1, lower boundary at 5.75 mbd) the sediments had a slightly lighter grey brown colour than in the darker coloured lower part (unit B.1.2.2). In both units patches of lighter coloured sediment, up to 5 cm long and 3 cm wide, were common. Further down, we divided the upper part of the *seqüència inferior* into two subunits. The upper part (unit B.2.1.1, lower boundary at 7.25 mbd) was very rich in light coloured phosphate patches, up to 1 cm in diameter. Also, orange and brown hydromorphic mottles were common. The lower part (unit B.2.1.2, 7.25–7.65 mbd) was characterized by light coloured patches and bands of phosphate as well as banded concentration patterns of iron hydroxide. The matrix was slightly darker than in the overlying unit. Unit B.2.2 of Soler and Maroto (1987a) was not exposed at the studied profile.

Sediment samples were taken continuously from 2.5 cm thick layers along a column about 20 cm in width (Fig. 2c). All sedimentological and mineralogical laboratory results described below were achieved on air-dried and dry-sieved samples of the fine earth fraction (particle diameters less than 2 mm). Prior to geochemical measurements, the sieved material was dried at 105 °C. Soil colour was measured for homogenized soil samples in triplicates with a spectrophotometer (Konica Minolta CM-5) by detecting the diffused reflected visible light in the 360 to 740 nm range under standardized observation conditions (2° Standard Observer, Illuminant C). The spectral information was converted into Munsell values and into the CIELAB Colour Space system (CIE 1976) using the Software SpectraMagic NX (Konica Minolta). The $L \times a \times b \times$ values indicate the extinction of light, or luminance, on a scale from $L \times 0$ (absolute black) to $L \times 100$ (absolute white), and express colour as chromaticity coordinates on red–green (a^*) and blue–yellow (b^*) scales. The redness rating index (RR) by Torrent et al. (1980) was calculated with Munsell values to describe changes in redness in the soil profiles as follows: $\mathrm{RR} = (10 - \mathrm{Hue}) \cdot \mathrm{Chroma} / \mathrm{Value}$.

Total carbon and nitrogen contents were determined on a subset of samples using elemental analysis (Vario EL of Elementar). Organic carbon was measured after destruction of carbonates with hydrochloric acid. Inorganic carbon contents were calculated by subtracting organic from total carbon. The loss of ignition (LOI) was determined from the gravimetric difference after heating at 105 and 1100 °C. Screening for volumetric magnetic susceptibility was accomplished by using a Bartington field spectrometer equipped with the MS2F sensor on sieved and homogenized samples.

Major and trace elements were analysed with X-ray fluorescence (Axios 3kW, PANanalytical GmbH) on pressed pellets. In order to derive geochemical indicators of post-depositional alteration by weathering, we calculated ratios of mobile to immobile elements (Na / Al, Ca / Ti, K / Rb) and the chemical index of alteration (CIA) according to Nesbitt and Young (1982): $\mathrm{CIA} = (\mathrm{Al_2O_3} / (\mathrm{Al_2O_3} + \mathrm{Na_2O} + \mathrm{K_2O} + \mathrm{CaO^*}) \cdot 100$. The $\mathrm{CaO^*}$ is referring to Ca included in silicates. $\mathrm{CaO^*}$ was estimated by subtracting the amount of Ca included in carbonates and phosphates from total Ca determined by X-ray fluorescence. Since the amount of Ca stored in these mineral groups may substantially vary with type and degrees of element substitution and crystallinity, we assumed that the percentage of Ca bound in carbonates and phosphates is equivalent to the percentage of inorganic C and phosphorus. This procedure may lead to overestimation of $\mathrm{CaO^*}$ and thus to underestimation of the CIA. The $\mathrm{CIA^*}$ value presented here is a relative measure of weathering degree, which should not be compared with previously published data.

The grain-size distribution was measured with a Laser Diffraction Particle Size Analyser (Beckman Coulter LS 13 320) calculating the mean diameters of the particles within a size range of 0.04–2000 µm with an error of 2 %. To remove the organic matter, the samples were treated with 0.70 mL 20 % $\mathrm{H_2O_2}$ at 70 °C for several hours. This process was repeated four times over a period of 2 days. To keep particles dispersed, the samples were treated with 1.25 mL $\mathrm{Na_4P_2O_7 \cdot 10H_2O}$ for 12 h (Pye and Blott, 2004; DIN ISO 11277, 2002). Two aliquots per sample were investigated in triplicates by an auto-prep station enabling equal measuring conditions. Each aliquot was measured two times to increase accuracy. To calculate the grain-size distribution the Mie theory was used (Fluid RI: 1.33; Sample RI: 1.55; Imaginary RI: 0,1) (Özer et al., 2010; ISO 13320-1, 1999).

For granulometrical and geochemical analyses, every second sample from the upper part of the sequence and every third sample from subunits of B.2.1 were used. The grain size distribution of samples taken from the upper part of the sequence was also measured after destruction of carbonates using 10 % HCl.

Semi-quantitative mineralogical data were obtained through X-ray diffraction (XRD) of powdered bulk samples using a Bruker AXS D8 Advance. The raw data were evaluated using Macdiff software (version 4.2.5). Mineral identifications were based on evaluations of prominent intensity peaks and the intensity of the main peak of each mineral used to calculate the percentage values (semiquantitative analysis). Diffractograms were prepared for a limited number of samples taken from all sediment units and from phosphate patches within unit B.2.1.1.

In addition, 7 sediment monoliths were extracted from selected parts of the sequence, from which 11 thin sections, 6 cm × 8 cm in size, were prepared by Th. Beckmann (Schwülper-Lagesbüttel, Germany). We preferentially sampled obvious and presumed interfaces between cultural levels

(Fig. 2c). The description of the thin sections follows Stoops (2003).

5 Results and discussion

The sedimentological and geochemical properties corroborate the subdivision in six sediment units observed in the field and suggest a further subdivision of unit B.1.1. The most prominent boundaries are between units A and B.1.1.1 at 2.25 mbd (Holocene finds to indeterminate Upper Palaeolithics) and between units B.1.2.2 and B.2.1 at 6.3 mbd (archaeological levels I and J with Mousterian occupation). Considerable data scatter within the units occurs. This is either related to differential precipitation of phosphate and iron hydroxides in the lower part of the profile, or to the heterogeneous nature of cultural layers, being locally enriched in bone or charcoal in the upper part.

5.1 Sedimentological parameters and magnetic susceptibility

The colour values a^* and L^* clearly delineate the sharp boundary at 6.3 mbd, below which a^* values strongly decrease towards less red colours and the luminance (L^*) substantially increases (Fig. 3). Luminance (L^*) is generally correlated to the amount of organic carbon or C_{org} (e.g. Schulze et al., 1993; Eckmeier et al., 2010) while redness is related to the presence of iron oxides (e.g. Scheinost and Schwertmann, 1999). Here, the colour values do not correlate with C_{org} or Fe concentrations, even when separated into the two main units. Plotting the relation of L^* to C_{org} and a^* to Fe confirms the separation of the profile at 6.3 mbd into two clearly defined groups (Fig. 4a and b). Although the upper part generally contains as much Fe as the lower part, the redness values are higher. As shown in Fig. 4c and d, the redness rating values are also higher. This, together with the ratio of $B^* - a^*$, is an indicator for the presence of hematite in the parts above 6.3 mbd which includes unit A. Lighter colours do not correspond to lower amounts of organic matter, especially in layers B.2.1 and B.2.2, although here additional factors have to be taken into account. The colours of sediments in unit B.2 are much lighter in comparison with unit B.1.1 where the amounts of C_{org} are similar. This could be explained by differences in sediment texture and higher proportions of sand in unit B.2, which is diluting the colouring effect of C_{org}. Another reason could be a difference in $CaCO_3$ content, but units B.2 and B.1.3 are both carbonate-free and sediments from unit B.1.3 are considerably darker. Above 6.3 mbd, the luminance values are the lowest in the profile, which correlate with a dark sediment colour described in the field and the elevated content of organic carbon (see below) in unit B.1.2.2. Several concomitant lows in a^*, b^* and L^* values at 2.83, 3.28 and 3.95 mbd correlate with elevated values of magnetic susceptibility. These peaks relate to comparatively dark lenses and sublayers, enriched with burnt residues and bone in archaeological levels C, D, and E. The scattering colour values in levels H and I (B.1.2.1) are probably related to lighter coloured patches and bands observed in the field, which may be caused by differential mineralization of organic matter or degraded limestone fragments. The gradual transition towards higher colour values at the uppermost part of B.1.1.1 and the transition from level B to the unit A corroborates the field observation. In the lowest part of the sequence, strong scatter of colour values is evident, which is related to the banded precipitation of iron hydroxide and phosphates observed in the field.

The contents of inorganically bound carbon considerably vary with depth, with a clear decreasing trend from maximum values at the top of unit B.1 equivalent to calcium carbonate equivalent (CCE) of 19.7 %, down to the base of unit B.1 and unit B.2.1, where inorganic carbon is only found in traces (CCE less than 1.0 %). These values reflect the same trend as reported by Kabiri (1993, Fig. 71, p. 135). Samples from unit A have CCE values between 3.9 and 4.9 % indicating that the fine fraction is not completely decalcified. Organic carbon is highest in the dark coloured sediments of unit B.1.2.2 with maximum values of 1.2 %. Minimum values of 0.1 % are recorded in the upper part of unit B.1 and in the light coloured sediments of unit B.2.1.1. The range of values compares fairly well with organic carbon values of Kabiri (1993, p. 133), which ranged from 0.25 to 1.37 %. The loss of ignition is between 6.0 and 14.6 % and shows similar trends as the inorganic carbon (correlation coefficient after Spearman $r_S = 0.863$, $\rho < 0.01$, $n = 78$). Total nitrogen varied between 0.045 and 0.245 % and maximum values are higher than those reported by Kabiri (1993, p. 133). Total nitrogen is closely related with organic carbon reflected in $r_S = 0.869$ ($\rho < 0.01$, $n = 78$). This may indicate that most of the N is included in organic molecules. The C / N ratio ranges from 4.1 to 8.9 showing considerable scatter in unit B.1.1 (data not shown). Kabiri (1993, p. 133) reported C / N ratios in between 3.37 and 6.4.

The magnetic susceptibility (Bartington field spectrometer, MS2F) ranges from 6 to 220 SI units with peak values in cultural layers (Fig. 3). The archaeological finds are locally concentrated in thin layers which often show peak values in magnetic susceptibility, probably owing to the presence of super-paramagnetic particles produced by burning, and which commonly correspond to darker colour and lows in luminance (L^*). The minimum values of magnetic susceptibility are found in units B.2.1. Here, processes of reduction and oxidation caused by fluctuating groundwater probably strongly reduced susceptibility values, as is known from hydromorphic soils (Evans and Heller, 2003). The peak value at 3.95 mbd, most likely, correlates with the maximum in magnetic susceptibility at about 3.8 mbd shown in Fig. 8 of Ellwood et al. (2001). The graph also shows cyclical change in magnetic susceptibility values which Ellwood et al. (2001) explained by differential weathering intensities related to

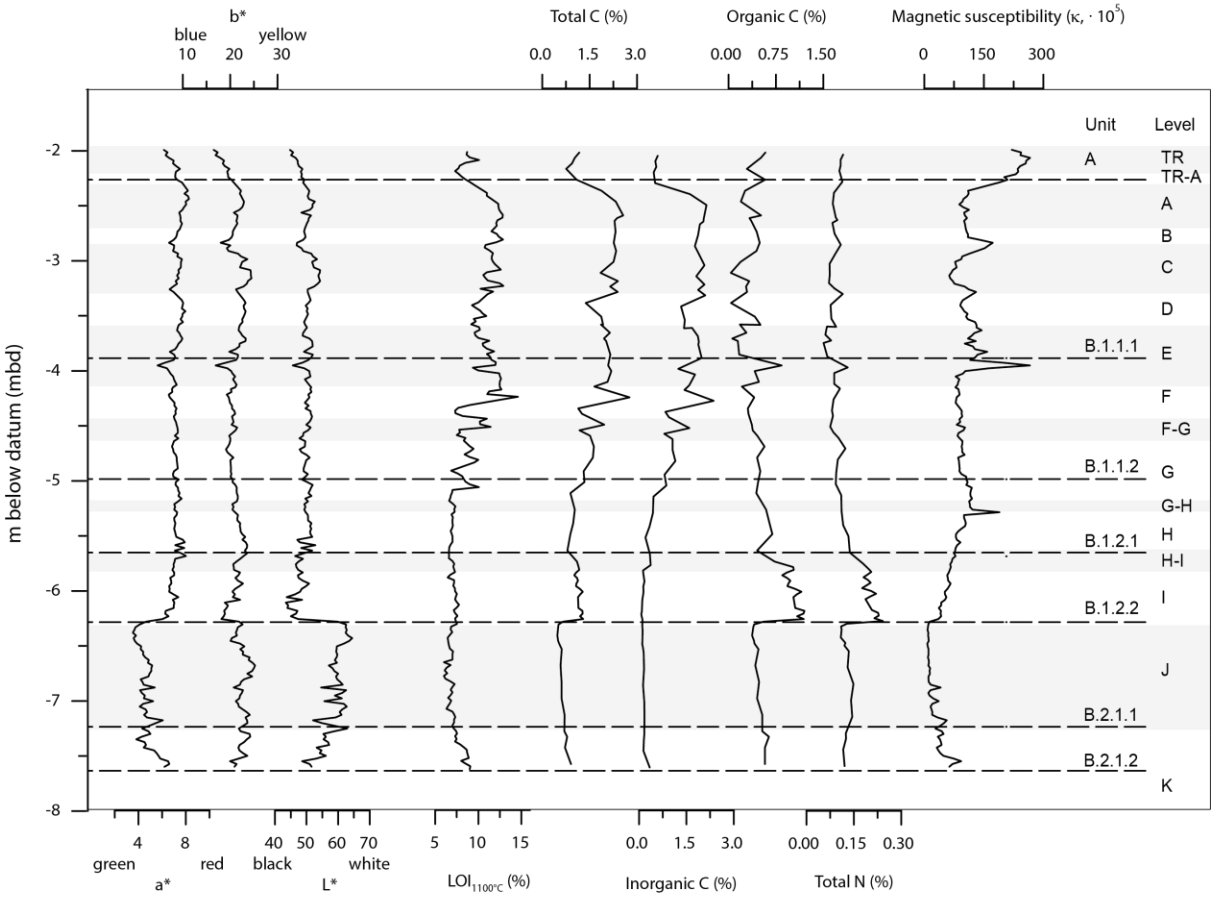

Figure 3. CIELab colour values, loss of ignition, total carbon and organic carbon, total N and magnetic susceptibility of the north profile at square E_0 at Arbreda.

temperature changes. This cyclicity is not clearly reflected in our data. Whether this absence is related to the sensitivity of measuring devices is difficult to assess, since the amplitudes of susceptibility changes are not quantified in the figure of Ellwood et al. (2001). Our data show a decrease in susceptibility values with depth in Aurignacian and Mousterian levels H to I, which was not discussed by Ellwood et al. (2001). We relate this decrease to an increasing influence of groundwater. Overall, using the magnetic susceptibility values as climate proxies for the E_0 sequence at Arbreda Cave would be misleading.

The granulometric analyses yields bi- or polymodal, often very poorly sorted grain size distributions (Fig. 5) indicating a polygenetic origin of the deposits. Silt is the dominant fraction in the upper part of the profile. Sand contents increase with depth in unit B.1.2.2 and sand dominates the lower parts of the sequence. Unit B.2.1.1 shows high contents of medium and coarse sand grains whereas the sand fraction of unit B.2.1.2 mainly consists of fine and very fine grains. In both units, sand grains are at least partly composed of phosphate and iron hydroxide concretions, which were not completely dispersed by sample pre-treatment. The amount of fine sand plus coarse silt grains, a size fraction prone to deflation and aeolian transport, ranges from about 40–56 % with highest amounts in samples from level I. Samples from this level also show low ratios between the 90th and the 10th percentiles (D90 / D10), hence a high degree of sorting. It thus appears that aeolian input was highest during accumulation of level I and in particular at the end of this phase. However, the same grain size fraction can be preferentially transported by sheet flow, which may have entered the cave. Sedimentary structures indicative of sheet flow, such as micro-laminations are, however, not evident.

In the stone-rich layers of unit B.1.1, strong scatter in sand and silt content, as well as poor sorting indicated by variable and high ratios of D90 / D10, are detected. The scatter may be related to variable amounts of primary carbonate grains and calcite cemented aggregates, but granulometric analyses after destruction of carbonates using HCl (10 %) shows that grain size of siliceous particles also varies considerably with depth in unit B1.1 (data not shown). This is interpreted as reflecting the detrital nature of the sediments in subunits of B1.1, which accumulated by roof-fall, infiltration by water, aeolian inputs and accidental transport into the cave.

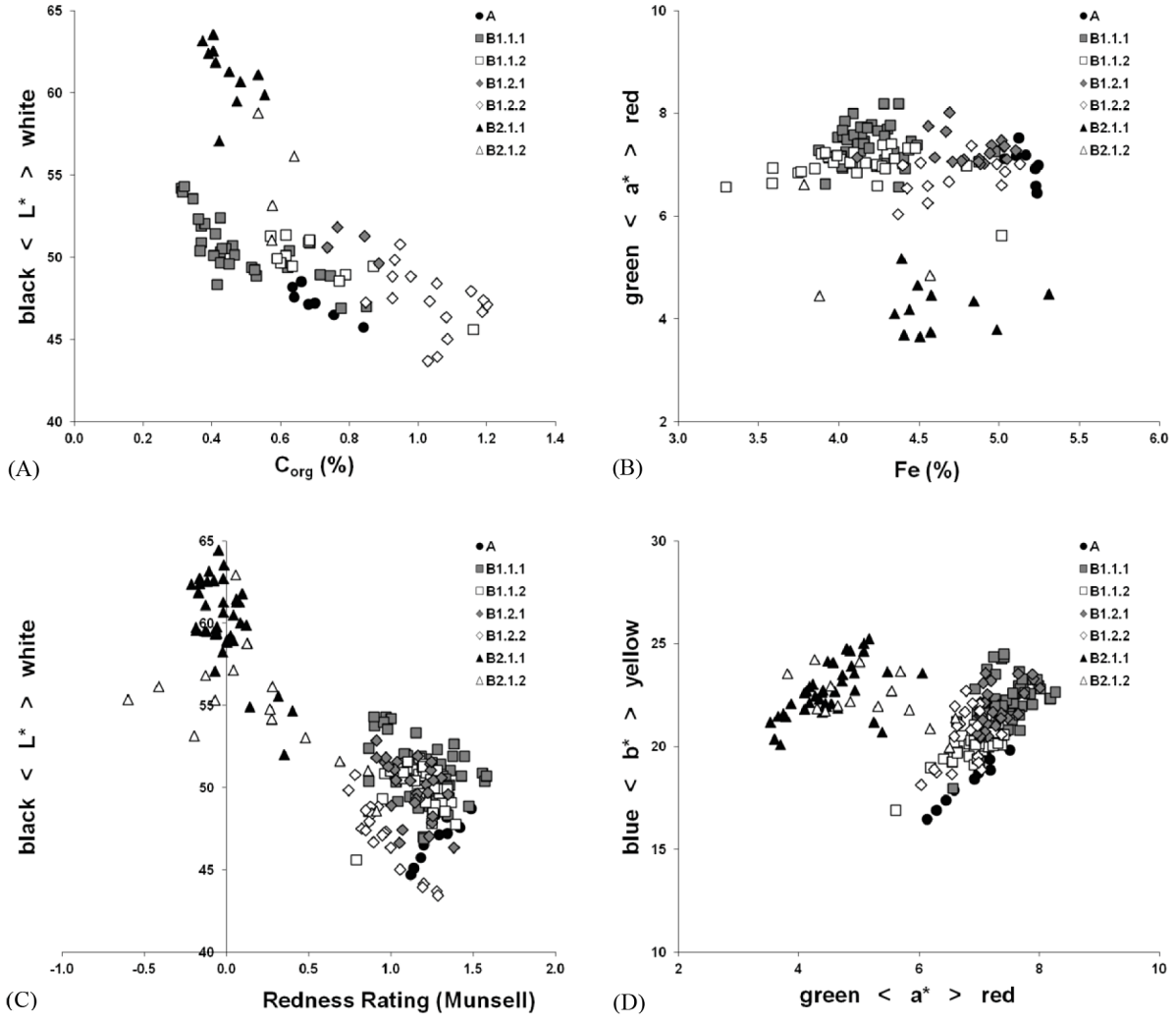

Figure 4. The colour values (CIE 1976) reflect the separation of the sediments into two main groups at 6.3 mbd. The luminance (L^*) and the organic carbon concentrations **(A)**, and also the redness values (a^*) and the iron concentrations **(B)**, do not correlate. The redness rating **(C)** and the relation of yellowness to redness **(D)** indicate differences in Fe oxide composition and, most likely, the presence of hematite in the sediments above 6.3 mbd, which includes the Holocene soil.

Samples from unit A shows highest clay contents of the sequence, probably relating to clay neo-formation in the Holocene soil and corresponding with comparatively high intensities of weathering in that level.

5.2 Mineralogy

The mineralogical composition is dominated by quartz in all sediment units (Fig. 6) ranging from 49 to 79 %. Feldspar and muscovite/illite, ranging from 6 to 11 % and 9 to 28 %, respectively, are minor components. Calcite attains maximum values in the upper part of the sequence. In the lower part of the sequence, the diffractograms suggest the presence of variscite ($Al[PO_4]_2H_2O$). Apatite/fluorapatite ($Ca_5[(F, Cl, OH)|(PO_4)_3]$) is detected in most samples. In the lower part, crandallite ($CaAl_3(PO_4)_2(OH)_5 \cdot H_2O$) occurs. Kabiri (1993, p. 120) reported that the K-bearing phosphate mineral leucophosphite ($KFe_2^{3+}(PO_4)_2(OH) \cdot 2H_2O$) amounted to about 7 % of the clay fraction in the lowermost layers. This mineral was also detected in one of our own samples.

The diffractograms for the phosphate patches in units B.2.1.1 and B.2.1.2 show the presence of crandallite and apatite besides quartz, feldspar and illite/muscovite (Fig. 6). Variscite is found in minor amounts as well.

Four different authigenic phosphates are detected in the sediment or in light coloured patches of it suggesting a complex paragenesis of secondary phosphate minerals in Arbreda Cave. Results of Kabiri et al. (1993) and our own measurements show a mutual presence of crandallite and apatite in

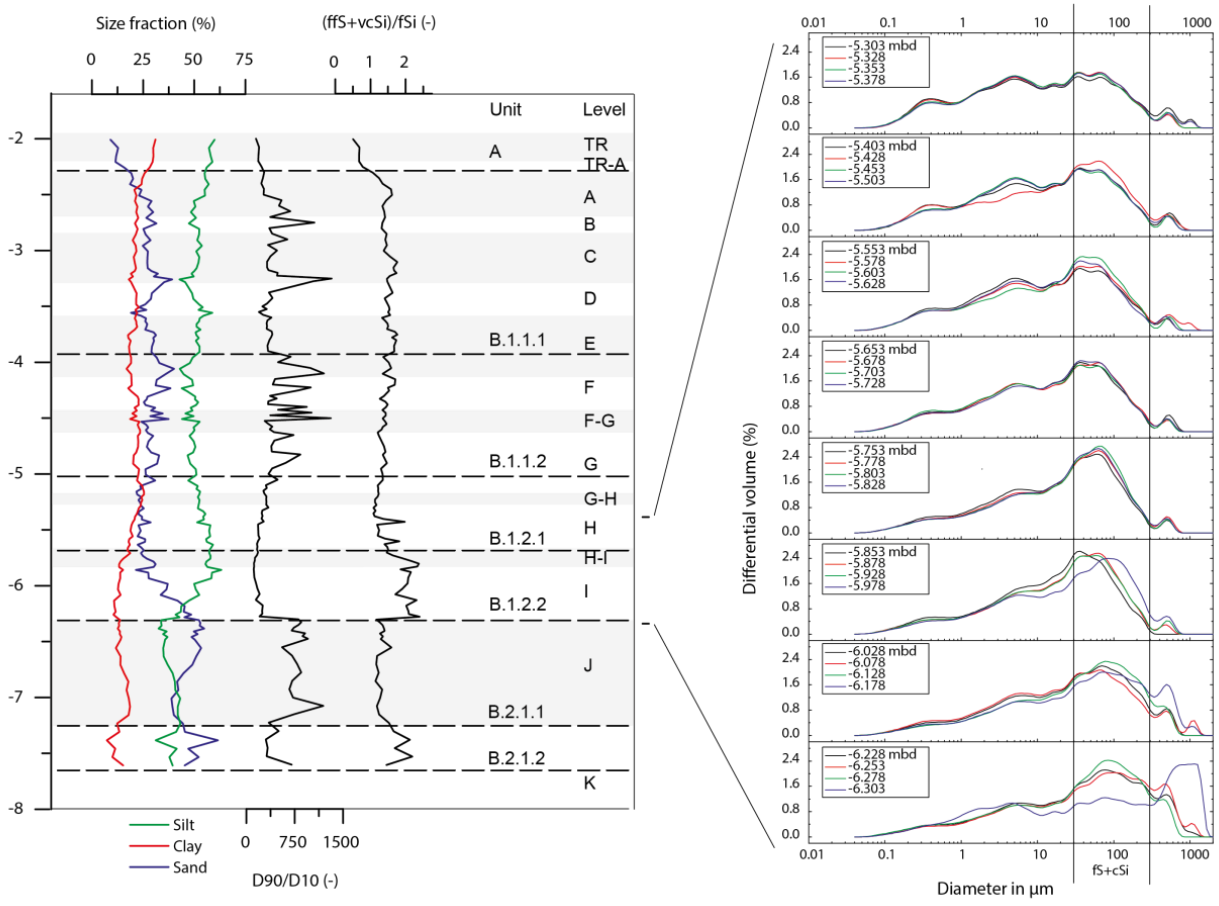

Figure 5. Granulometrical parameters of the fine fraction (< 2 mm in diameter) and frequency distributions for samples from the MP/UP transition of the north profile at square E_0 at Arbreda.

the lower layers. These minerals have different stability fields (Karkanas, 2010), i.e. crandallite is stable at pH values of 6 to 7, whereas apatite occurs above pH 7. According to our measurements of selected samples taken from the whole sequence, pH ranges from 7.4 to 7.9 as measured in a 1 : 2.5 sediment/water extract (data not shown). The presence of both minerals could indicate that pH was lowered in former times when crandallite formed and pH subsequently rose by addition of bases through groundwater flow. Reaction of phosphate-rich leachates with Al-rich sediments and precipitation of variscite (Onac et al., 2004) may add to this picture. In order to verify these hypotheses more detailed analyses would be needed.

5.3 Major and trace elements

The geochemical composition is dominated by Si (18.74–26.87 %), Al (6.23–10.05 %) and Ca (1.68–14.27 %). In the upper part of the sequence, Si and Al as well as K (1.64–2.90 %) and Ti (0.35–0.55 %) show very similar behaviours (Fig. 7), which probably relates to their common occurrence in siliceous minerals such as feldspar and phyllosilicates. In the lower part of the sequence, these elements are not in close relation with each other (Fig. 7). Calcium, being a main component of carbonate rocks and minerals, is negatively correlated with the siliceous elements, while Mg (0.25–1.19 %), which may be found both in phyllosilicates and dolomitic limestone, decreases with depth. Iron (Fe, 3.14–5.10) is slightly enriched in unit A and below about 5 mbd. In contrast, Mn (0.01–0.36 %) has minimum values in this depth, but shows a strong increase in the lowermost strata. The P values peak at around 2.80 and 3.30 mbd and strongly increase at 3.90 mbd, i.e. at depths where the sediment was comparatively dark (lower L^* values), and shows peak values in magnetic susceptibility. The rise at 3.90 mbd is also reflected by Zn and Cu (Fig. 8) and is probably related to increased zoogenic inputs. The extent to which human faeces contributed to phosphorus and trace element inputs is not clear. To our knowledge it is not possible to distinguish between element inputs by humans and other mammals. Bone fragments and fragments of carnivore coprolites occur in the respective depth, as observed in thin sections CA5, CA6 and CA7. There is no direct microscopic evidence, however, of human faeces. Evidence for defecation by humans and a

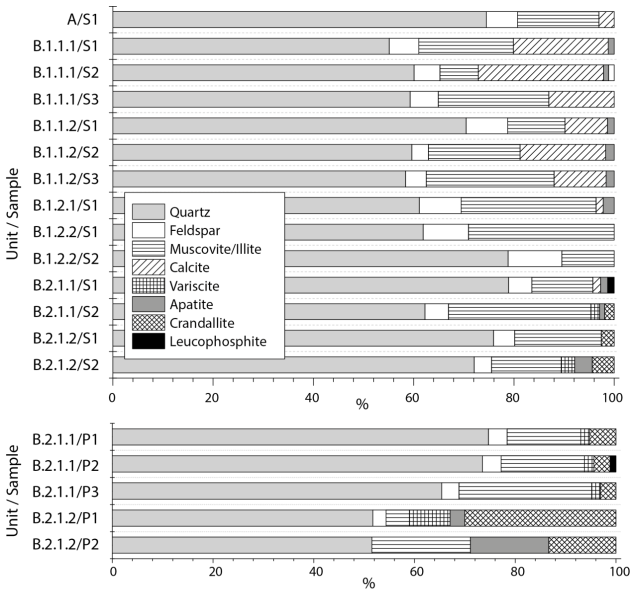

Figure 6. Mineralogical composition in selected samples from different sediment units (upper) and selected phosphate patches (lower) of the north profile at square E_0 at Arbreda.

distinction between anthropogenic and other zoogenic inputs may be gained from faecal biomarker analyses (e.g. Sistiaga et al., 2014).

The P contents increase further with depth, and strongly rise below the sharp sediment boundary at 6.3 mbd. In units B.2.1.1 and B.2.1.2 there is considerable variation in P values.

The sharp geochemical boundary at 6.3 mbd is also delineated by the trace elements Cu, Pb and Ni (Fig. 7), as well as Co and La (data not shown) which strongly drop below the boundary to levels equal to (Cu) or considerably below (Ni) the minimum values recorded in the sequence above the boundary. The low Ni concentrations and comparatively high Zr concentrations of unit B.2.1.1 appear to suggest that sediment source changed across the boundary between units B.2.1.1 and B.1.2.2. However, higher Zr correlates with coarser grain sizes, and Ni concentrations may be affected by mobilization and leaching with fluctuating groundwater. In all subunits of B.1, above the boundary, Cu shows a close relation with P suggesting a common source for both elements; probably bat guano or mammal faeces. Significant decreases in P and Cu across the boundary of levels I and H document reduction in zoogenic inputs during the transition from final Mousterian to Archaic Aurignacian. This does not necessarily imply an increased human presence at the beginning of the Upper Palaeolithic.

Strontium values strongly increase across the boundary at 6.3 mbd from values below 400 to about 2400 mg kg^{-1}, reaching much higher concentrations than usually found in soils or sediments (Kabata-Pendias, 2011, p. 42; De Vos and Tarvainen, 2006). Strontium has a similar geochemical behaviour as Ca and Ba; however, in our data set, Sr is related neither to these elements nor to clay minerals or organic matter in which Sr can be incorporated and preserved from leaching. Tertiary marls and evaporites may have high Sr contents, and as it is geochemically mobile, Sr in Arbreda Cave could originate from groundwater seeping out of the travertine terrace and the marls located to the west of the Serinyadell valley (Fig. 1c). In that case, a concomitant enrichment with Ca should be expected, which was not the case. Also, groundwater seepage would not explain the abrupt increase at the boundary. Since there is a close correlation of Sr with P ($r_S = 0.72$, $\rho < 0.01$, $n = 22$) in unit B.2.1, it is more likely that Sr originates from zoogenic inputs.

Across the boundary at 6.3 mbd, a considerable rise in K is also recorded. The increased K values are difficult to explain since neither phyllosilicates nor feldspar shows a concomitant enrichment. Instead, higher sand contents and coarser median grain size go along with augmented quartz contents. This granulometric effect is also reflected by Zr values increasing in the lower part of the sequence. The occurrence of leucophosphite as detected by Kabiri (1993) may contribute to but not fully account for increased K values.

Over the whole profile, the minor variations in geochemical ratios of Ti / Zr, Al / Ti and Fe / Al (Fig. 8) do not indicate major changes in source area of fines over time. Differential intensities of carbonate leaching in units A and B.1 are reflected in the Ca / Ti ratio. Although CCE values were below 1 % in the lower part of the sequence, Ca contents and the Ca / Ti are higher than in unit A because considerable amounts of Ca may be bound in phosphates. The Ca / Mg ratio increases considerably from unit A towards unit B, where the ratio is fluctuating around 10 with a considerable scatter. Geochemical ratios of mobile to less mobile elements such as Na / Al, Si / Al, K / Rb or Sr / Ba indicate higher weathering degrees for samples taken from unit A than for those of other units. This is reflected by the CIA* values (Fig. 8). Low degrees of weathering are indicated for the central part of the sequence comprising subunits of B.1.1. High concentrations of K and high K / Rb ratios in unit B.2.1.1 suggest low weathering degrees, whereas the Si / Al ratios and the CIA* values indicate higher weathering degrees. Also, heavy mineral spectra as reported by Kabiri (1993) for the lowest part of the sequence were comparatively rich in the weathering-resistant minerals zircon and tourmaline, whereas instable minerals such as augite or epidote, being common in the other units, were virtually absent. This was interpreted as a clear indicator of higher degrees of weathering below about 6.3 mbd. However, Kabiri (1993) found that in the corresponding depth at the south profile of sector alpha, the unstable minerals are still present. It was concluded that this difference is related to local guano inputs to the sediments of the north profile, whereas the south profile received secondary phosphate by phosphate-rich lateral or vertical flow.

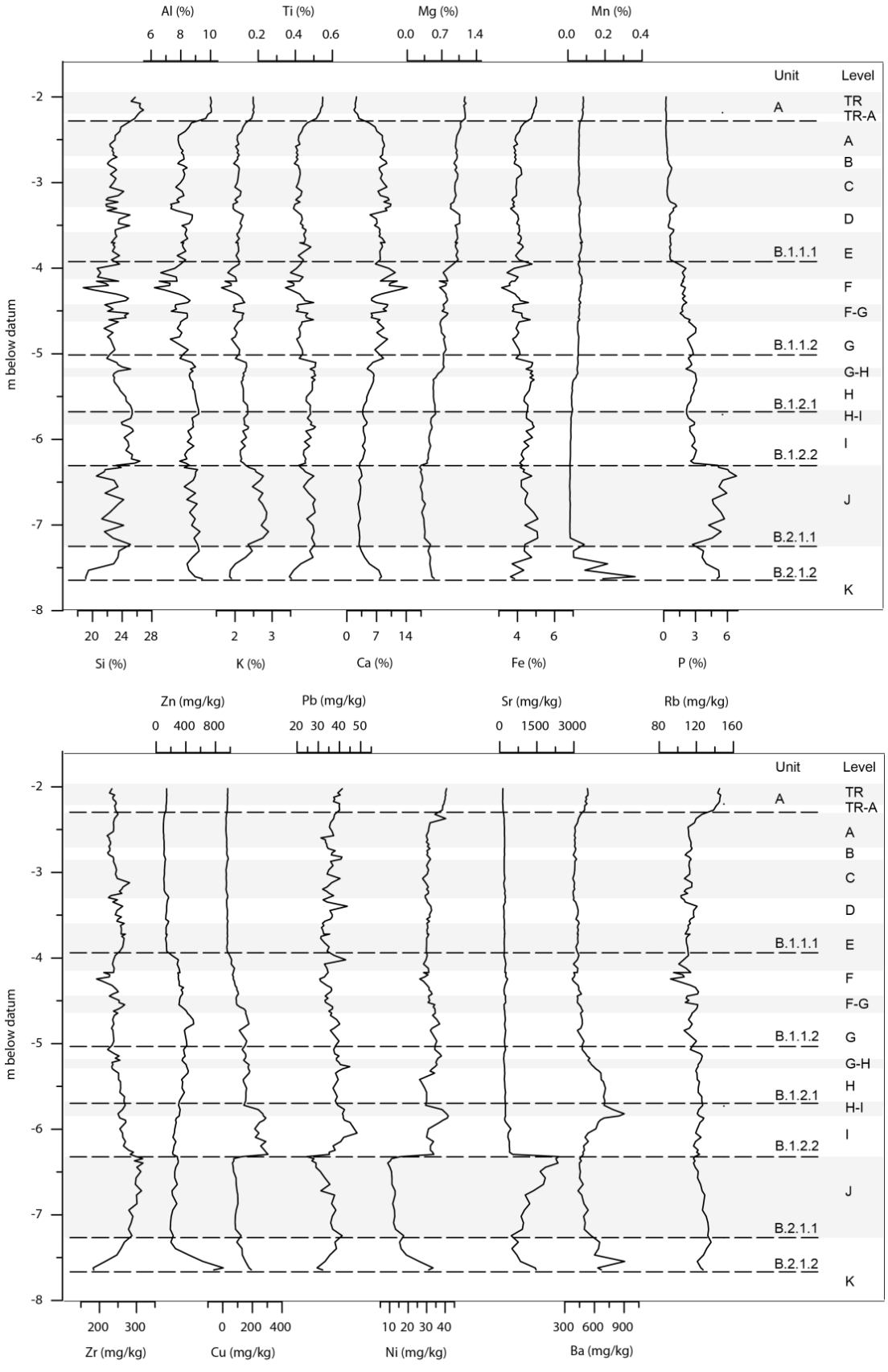

Figure 7. Major and trace elements in the fine fraction (< 2 mm in diameter) of the north profile at square E_0 at Arbreda.

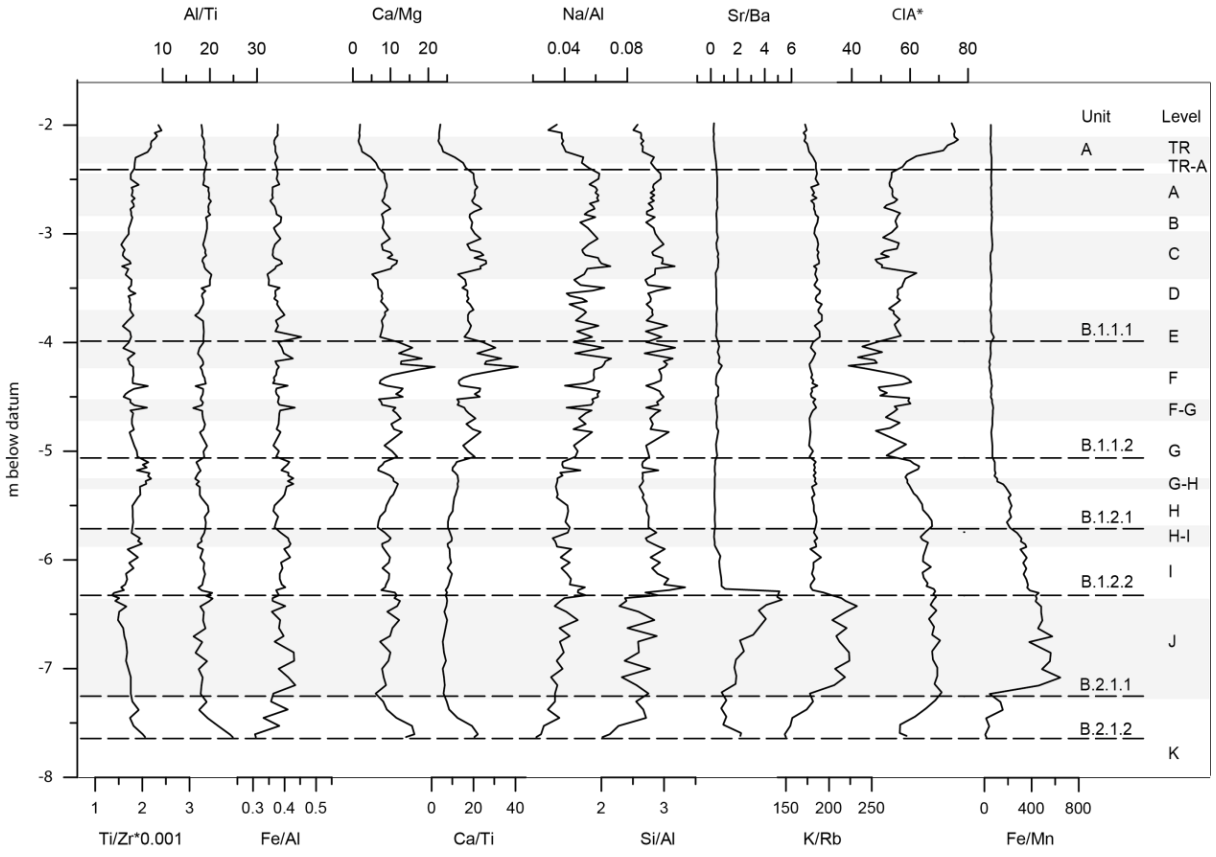

Figure 8. Geochemical ratios for the fine fraction (< 2 mm in diameter) of the north profile at square E_0 at Arbreda.

The ratio of Fe / Mn displays a strong relative Mn depletion starting from below about 5 mbd towards the base of unit B.2.1.1 at 7.25 mbd; from here Mn values again rise with depth. Intense mottling shows that part of the iron was reduced and transported as ferric iron and later precipitated as hydroxides. Frequent reduction and oxidation reactions produce hydronium ions, which may cause dissolution of carbonates and lowering of pH. If this has been the case in unit B.2.1.1, pH afterwards increased to the present values of about 7.6. Heavy mottling suggests the presence of groundwater or interflow during or after deposition of level J. While iron was still present, manganese, geochemically more mobile than iron, has almost completely leached from this layer. Further down the profile, dark bands of Mn occur. Their presence could be related to a lower groundwater table in the valley during the incision of Serinyadell River. Alternatively, seepage from the travertine terrace could transport dissolved Mn to the cave.

The possible effects of groundwater and lateral flow have to be taken into account in future radiometric dating efforts, since it is likely that radiometric equilibrium is not given in sediment units B.2.1.1 and B.2.1.2.

5.4 Micromorphology

The micromorphological investigations show major differences between the upper part of the sequence including thin sections from monoliths CA-MM7 to MM4, and the lower part with thin sections from monoliths CA-MM3 to MM1 (Fig. 9). In the upper part, the coarse fraction consists of mono- or polycrystalline quartz, as well as calcite, feldspar and mica grains. Most rock fragments are composed of travertine but few limestone fragments occur as well. The fragments are irregularly shaped, but have round edges probably related to post-depositional weathering. Angular shapes with acute-angled faces that would indicate frost shattering are very rare. In the lower part of the sequence, calcite grains are absent and travertine fragments occur only in thin section CA-MM3.1. This corresponds well with very low CCE contents measured for the lower part of the sequence.

The very few sandstone or quartzite fragments detected are all well rounded and probably originated from the flood plain of the Serinyadell River and were brought inside the cave by humans. Very rarely, fine flakes of flint, up to 5 mm in length, are present (Fig. 10a and b).

Bone fragments (Fig. 10c and d), mostly of small size, occur in diverse states of burning and preservation. Bone is

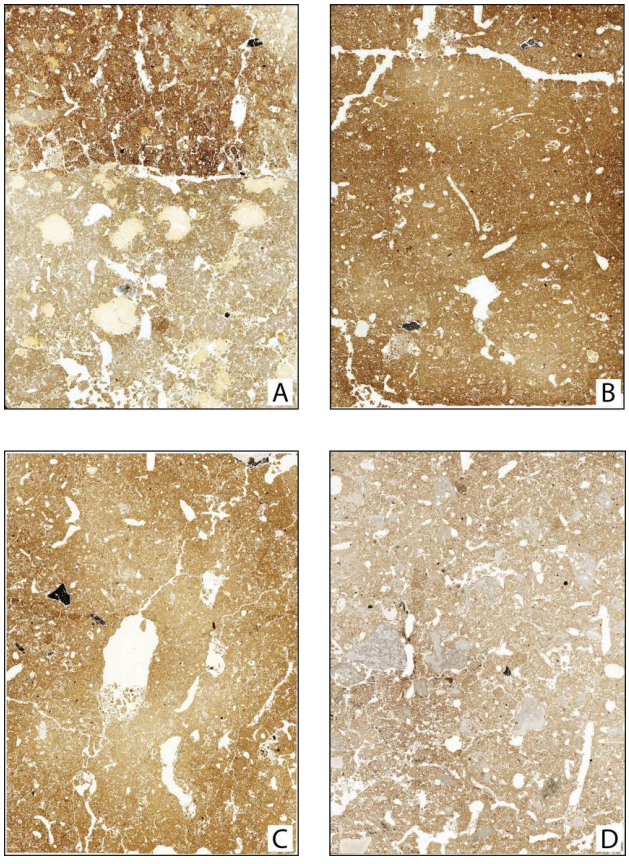

Figure 9. Flatbed scans of selected thin sections prepared from the sequence at Arbreda Cave. **(A)** CA-MM1 contains the sharp erosional contact between archaeological levels J and I equivalent to sediment units B.1.2.2 and B.2.1.1. The difference in groundmass colour and between types and sizes of phosphate infillings is clearly visible. **(B)** CA-MM2.1 from sediment unit B1.2.2, **(C)** CA-MM2.4 from sediment unit B1.2.1 and **(D)** CA-MM7 from sediment unit B.1.1. The frame width equals 6 cm. (Further explanations see text.)

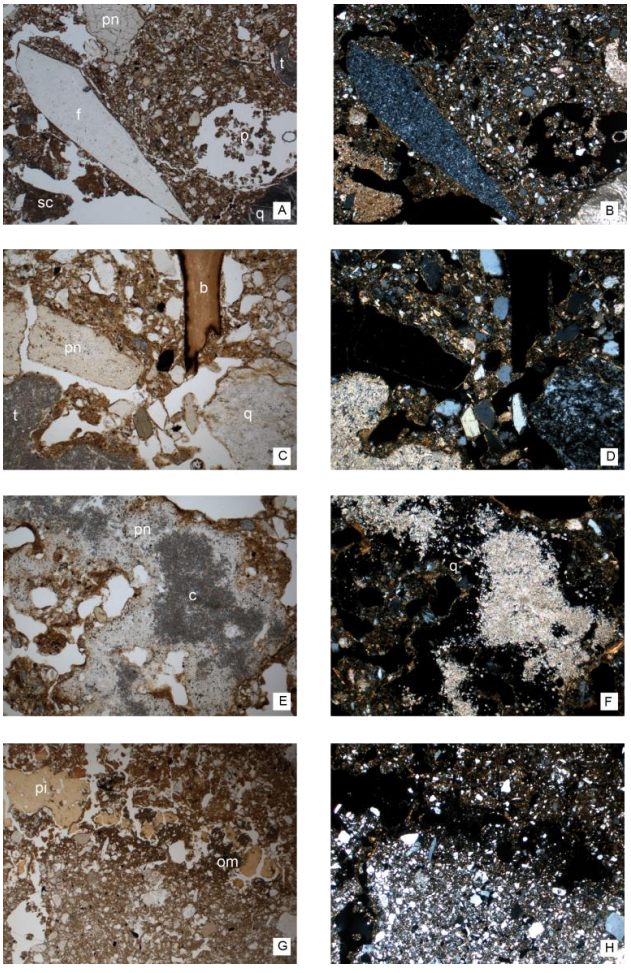

Figure 10. Micrographs from Arbreda Cave. **(A)** Flint (f), travertine (t) and quartzite (q) fragments, phosphate nodule (pn), secondary calcite (sc) and large biopore in thin section CA-MM7 from sediment unit B1.1 (plain polarized light (PPL), frame width is $\sim$ 5 mm). **(B)** Same as **(A)** but crossed polarizers (XPL). **(C)** Partially burned bone (b), quartzite (q) and travertine (t) fragments, phosphate nodule in thin section CA-MM7 (PPL; frame width $\sim$ 1.25 mm). **(D)** same as **(C)**, but XPL. **(E)** phosphate nodule (pn) with intergrowth of micritic calcite (PPL; frame width $\sim$ 1.25 mm). **(F)** Same as **(E)**, but XPL. **(G)** phosphate infillings (pi) and organic matter (om) at the boundary between levels I (upper part) and J (lower part) in thin section CA-MM1 (PPL; frame width $\sim$ 5 mm). The light orange P infillings on the right-hand side are probably stained by organic matter. **(H)** same as **(G)**, but XPL.

common in the upper part of the sequence, whereas very few pieces are observed in the thin sections from the lower part. Charcoal fragments occur in most thin sections. There was no clear indication of burnt soil. In thin sections CA-MM6 and 7, clusters of highly birefringent calcite crystals are locally associated with fine charcoal flakes. These crystals resemble ash calcite, but they are difficult to distinguish from secondary calcite as found in incomplete infillings. Overall, there is a scarcity of burned features in the studied thin sections. This should be interpreted with care, since thin sections were not taken from the central part of the archaeological levels.

The pore space mainly consists of frequent channels, chambers and burrows, whereas complex packing voids and planes are less common. Chamber or burrow microstructures are dominant. Ped development is rather limited, but locally a moderately well-developed subangular blocky microstructure is expressed, e.g. at the lower boundary of archaeological level I in thin section CA-MM1. In addition, granular microstructure and circular aggregates are occasionally found. These, in combination with the high frequency of biogenic pores, suggest that formation of secondary structure was related to biological activity.

Thin sections from the lower part of the sequence show a higher degree of compaction than those from the upper part. In the central part of thin section CA-MM2.1, sub-horizontal

alignment of compacted sediment is visible which probably resulted from trampling. Large biogenic pores are not deformed, since they were formed after compaction. At the upper boundary of the contact level between the final Mousterian and Archaic Aurignacian levels J and I in thin section CA-MM2.4, several discontinuous patches of finely laminated sediment, about 2 mm thick, are present. These resemble fragments of sedimentary seals (Pagliai and Stoops, 2010), which indicate redistribution of fines by surface runoff or infiltrating water. There was no indication of frost effects such as silt cappings, grain sorting or lenticular peds (Van Vliet Lanoë, 2010).

The birefringence fabric of the light brown to dark brown groundmass is stipple-speckled to weakly developed mosaic-speckled in all thin sections, whereas light coloured patches within the groundmass of the lower half of CA-MM1 show an undifferentiated b-fabric, and crystallitic b-fabric occurs in carbonaceous groundmass of thin sections CA-MM5–MM7.

Further features of the thin sections relate to phosphate. Typical cryptocrystalline phosphate nodules of light grey colour (PPL, black under XPL) with brown or grey dots and inclusions of silt size mineral grains are present in all thin sections. Most of these nodules have diameters in the sand fraction, sharp edges and a dense fabric. Locally, dirty phosphate infillings with black (PPL) and milky (XPL) patches are found. We assume that these nodules represent fragments of small rodent or carnivore coprolites. In the upper part of the sequence, these nodules include highly birefringent submicroscopic calcite crystals, which appear to grow on the isotropic phosphate (Fig. 10e and f). These intergrowths probably relate to diagenetic changes.

In the lower part of the sequence, two types of jellylike phosphate infillings (Fig. 10g and h) are abundant to very abundant. Type 1 consists of orange brown incomplete infillings, up to 3 mm in diameter, commonly with shrinkage cracks due to desiccation and/or partial solution. The brown colour probably relates to staining by organic acids and/or Fe hydroxides. Type 2 are light yellow, mostly complete infillings which exclusively occur in the lower half of thin section CA-MM1, representing the uppermost part of sediment unit B.2.1.1. These infillings are much larger, up to 10 mm in diameter, and are in a better state of preservation than those of type 1. The type 1 infillings probably represent bat droppings, which were partly degraded and transformed, whereas the type 2 infillings were precipitated from solution. The phosphate source of type 2 infillings may have been degraded guano or urine. Below the sharp boundary at 6.3 mbd in sediment unit B.2.1.1 frequent water saturation and lack of organic matter may have promoted the precipitation and preservation of inorganic phosphates.

Other pedofeatures consist of calcite hypocoatings and incomplete infillings observed in thin sections CA-MM4–MM7. These calcitic pedofeatures testify to carbonate dissolution and precipitation in the upper part of the sequence. Dusty clay coatings, less than 100 µm thick, occur throughout.

Across the boundary from Late Mousterian to Archaic Aurignacian, charcoal and flint particles are very rare. This scarcity of anthropogenic materials in profile E_0 suggests that during the transition from Middle to Upper Palaeolithic the cave was rarely occupied by humans. This hypothesis is discussed further below.

5.5 Implications for site formation, climate and human occupation

Overall, the stratigraphical distinction in sedimentary field units is corroborated by changes in colour, granulometric composition and contents of major and trace elements.

The lower part, unit B2.1, has a unique sedimentological and geochemical fingerprint. It is very likely that it accumulated by fluvial deposition (Table 1) when the altitudinal difference between the cave mouth and the former floodplain of the Serinyadell was smaller than today. During periods of flooding, the creek might have entered the cave and deposited fines. During or after deposition, precipitation of iron hydroxides occurred, indicated by intense mottling. We hypothesize that this mottling took place under the influence of a shallow groundwater table, related with the former floodplain of Serinyadell River. Enrichment with Mn, detected in the lowermost part of unit B2.1.2 probably occurred during a later phase of post-depositional transformation and was related to seepage from the travertine terrace. At a later stage, intense P enrichment from vertical percolation and possibly lateral flow of P-rich pore waters took place. The source of P is bat guano or urine of mammals such as cave bear or hyaena whose presence at that time is documented by faunal remains (Estévez, 1997; Soler et al., 2012). The discontinuity between Mousterian levels J and I is marked by most sedimentological, geochemical and micromorphological parameters and is probably erosional. It covers a sedimentary hiatus of unknown duration. P enrichment continued after part of the fluvial deposit was eroded and buried under the silty deposits of level I. Enrichment with geochemically mobile Sr relates to the same mechanisms, zoogenic inputs being the most probable source.

Sediment composition slightly changes from Late Mousterian level I to Early Upper Palaeolithic level H and G, the latter being characterized by lower contents in Cu, fine sand and coarse silt, and by a lighter colour. Although micromorphology gives evidence for local reworking at this boundary, other data presented suggest a rather gradual transition than a sudden change between the two levels.

The geochronological control for the deposition of levels I and H is mainly based on a set of accelerator mass spectrometry radiocarbon ages published by Bischoff et al. (1989), Soler and Maroto (1993) and Maroto et al. (1996, 2012). The corresponding ages show a considerable overlap of intervals at the 95.4 % probability level (Fig. 11), but the results on

Table 1. Relative significance of selected accumulation and alteration processes in the north profile of square E_0 and correlation with the pollen zones and climate reconstructions of Burjachs and Renault-Miskovsky (1992, Fig. 3). The P enrichment is related to zoogenic inputs. Anthropogenic accumulation of lithics, bone or charcoal is low over the whole sequence, but find densities at Arbreda spatially varies.

		Sediment accumulation				Sediment alteration			Pollen (Burjachs and Renault-Miskovsky, 1992)		
Sediment units	Archaeo-logical levels	Fluvial	Aeolian or sheet wash deposits	Rock fall	Collu-vial	Iron mottling	P-enrich-ment	Secon-dary carbo-nate	Archaeo-logical levels	Pollen zone	Inferred climate
A	*Terra rossa*	–	+	(+)	++	–	–		Postpal.	10	Warm and humid
B1.1.1	A, B, C, D, E upper	–	+	++	–	–	+	*	A	9–10	Cool and humid
										8–9	Temperate and humid
									B	7–8	Cold and dry
									C	7	Cold and dry
									D	6–7	Cold and dry
									E	6	Cool
B1.1.2	E lower, F, G upper	–	+	+++	–	–	++	*			
									F	5	Cold and dry
									G	4	Temperate and humid
B1.2.1	G lower, H	–	++	+	–	–	++			3	Cold and dry Cool and humid
									H	2	Temperate and humid Cold and dry
B1.2.2	I	–	++	–	–	–	++		I	1	Temperate and humid Cold and dry Temperate and humid
B2.1.1	J	+++	–	–	–	++	+++				
B2.1.1	K	+++	–	–	–	++	+++	*			

Ratings: – insignificant, very weak; + low, weak; ++ moderate; +++ high, *: Presence of secondary carbonates as deduced from field study and micromorphological investigations.

bone samples only (OxA 3729, OxA 3730, and OxA 3731, Maroto et al., 1996) reflect the expected trend of increasing age with depth. The validity of these ages were questioned by Zilhão and d'Errico (1999, 2000, 2003) and Zilhão (2006) who claim that sedimentological boundaries between the levels are not well defined due to bioturbation and that stratigraphic context of samples is insufficient to provide reliable age estimates. Soler et al. (2008) discussed the doubts from the perspective of the excavators and presented two plots of find distributions along W/E and N/S profiles, which document separation into two distinct archaeological levels. New geochronological studies in Central and Southern Iberian cave sites (Wood et al., 2013; Kehl et al., 2013) suggest that previous radiocarbon datings most probably underestimated the time of late Neanderthal occupation. Recently, statistical overlap in radiocarbon dates was observed for Late Middle Palaeolithic (LMP) and Early Upper Palaeolithic (EUP) layers at Cova Gran, although these layers are separated by an archaeologically sterile sediment (Martínez-Moreno et al., 2010). However, recent new datings for Arbreda show that radiocarbon ages for the Archaic Aurignacian and Late Mousterian may have been overestimates (Wood et al., 2014). These examples suggest that results of the radiocarbon method should be interpreted with care and independent age control is needed to verify the time frame for the LMP/EUP transition at Arbreda.

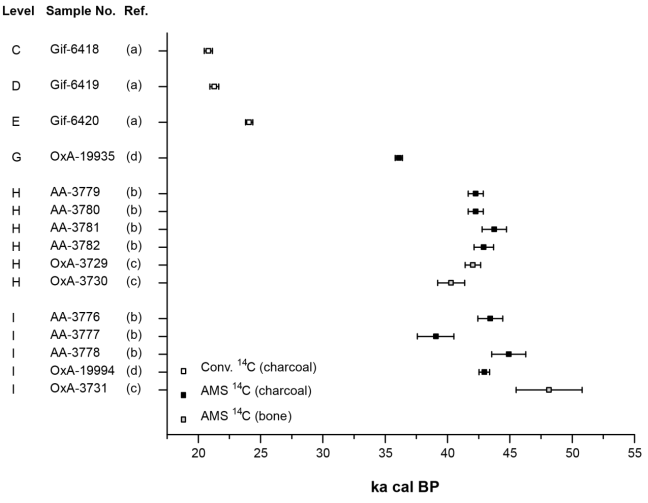

Figure 11. 95.4 % probability interval of calibrated ^{14}C ages of charcoal and bone samples after **(a)** Delibrias et al. (1987), **(b)** Bischoff et al., 1989, **(c)** Maroto et al. (1996) and **(d)** Maroto et al. (2012). The laboratory protocols used by Maroto et al. (2012) include rigorous sample pre-treatment to minimize contamination of samples. For calibration the CalPal-2007-Hulu data set (Weninger and Jöris, 2008) and the CalPal software package (Weninger et al., 2008) were used.

High contents of potentially wind-blown grain sizes suggest aeolian input during deposition of level I. This can be

interpreted as an indication of dry climate, because aeolian deflation may be enhanced during periods of reduced vegetation cover. The dry phase may have correlated with the cold and dry period that occurred during accumulation of level I as postulated from pollen data (Burjachs and Renault-Miskovsky, 1992), and with the onset of aeolian deposition reported for layer A at Abric Romaní (Courty and Vallverdú, 2001). The climate signal extracted from our data at Arbreda, however, is not well constrained and other sedimentary features reflecting signals of climate change, such as increased proportions of frost-shattered rock fragments, microscopic silt cappings or cementation by calcite (e.g. recorded at El Bajondillo; Bergada and Cortés-Sánchez, 2007; Cortés-Sánchez et al., 2008) were not identified. The frequent changes in climate postulated from pollen analyses (Burjachs and Renault-Miskovsky, 1992, Fig. 3) are not reflected in our sedimentological and geochemical data. However, the general trend of climate worsening from Middle to Late Upper Palaeolithic is mirrored by the sediment properties discussed in this paper, e.g. by an increase in CIA* values reflecting increased weathering in units B1.2, B2.1.1 and A.

The sediments of the Upper Palaeolithic levels of Arbreda have mainly accumulated by rockfall, aeolian deposition or accidental transport into the cave. There is no clear evidence for transport by sheet flow, but related sediment structures such as laminations may not be preserved due to bioturbation. P enrichment is less intense than in lower levels. Carbonate metabolism led to the formation of secondary carbonate reflecting limited leaching. There is no clear evidence of increased freeze–thaw, which may indicate limited cooling and/or dry climate conditions. Anthropogenic materials occur in patches between large boulders of travertine.

The low amounts of archaeologically relevant materials including charcoal and flint in sediments from levels I and H apparently point to rare occupation of the cave during the MP/UP transition. In fact, archaeological levels at Arbreda are often separated from each other by archaeologically impoverished spaces and travertine blocks (Soler et al., 2008, p. 52). However, the density of finds in Arbreda shows considerable lateral and spatial variability. In several squares, levels H and I are both rich in finds and there is no evidence for a gap in occupation (see Figs. 3 and 4 in Soler et al., 2008). Most cave sequences of the Iberian Peninsula, which document the MP to UP transition, contain intercalated archaeologically sterile layers or sedimentary disconformities and discontinuities (Mallol et al., 2012), clearly reflecting periods of non-occupation or at least major changes of the depositional system. The sequence at Arbreda Cave thus appears to be the exception rather than the rule. If we accept the notion of continuous occupation at Arbreda, and postulate a common arrival of anatomically modern humans, Arbreda would document one of the latest occupations of Neanderthals in Northern Iberia. However, considering the subtle evidence of sediment disconformity in the E_0 profile and find distributions presented in Soler et al. (2008), discontinuous occupation at Arbreda appears to be more likely.

6 Conclusions

The analytical data derived from this multiproxy study refine the previously presented macroscopic subdivision and give new evidence on site formation processes in this key sequence regarding the study of cultural changes during the Middle to Upper Palaeolithics in NE Iberia.

The sediments of levels K and J were deposited by fluvial processes and affected by groundwater or interflow, whereas the remainder of the Palaeolithic sequence accumulated by rockfall, slabbing off the cave wall and detrital inputs of fines.

Weathering degrees deduced from geochemical parameters show a trend of climate worsening which correlates with climate reconstructions by palynological data. We could not identify well-constrained phases of abrupt climate change, as reported from the study of other cave sequences and geoarchives in the Iberian Peninsula. This is at least partly related to insufficient temporal resolution of the sequence. There is, however, evidence for increased aeolian inputs during the Late Mousterian, which was probably followed by a period of infrequent occupation of the cave. These phenomena may be linked with climate worsening during a stadial phase of MIS3.

Correlation of the sequence with climate records of closeby geo-archives such as Lake Banyoles may be facilitated if age control on sediment deposition can be improved.

Acknowledgements. We gratefully acknowledge granulometric analyses by Jens Protze and Marianne Dohms (Chair of Physical Geography and Geoecology, Department of Geography, RWTH Aachen University, Germany). Sven Berkau (Steinmann Institute for Geology, Mineralogy and Palaeontology, University of Bonn) carried out mineralogical analyses. We thank the German Research Foundation for financial support for project C1 of the CRC806 Our Way to Europe.

Edited by: F. Viehberg

References

Alcalde, G.: El rossegadors del Paleolític superior de la Cova de l'Arbreda (Catalunya), Significació paleoecològica i paleoclimàtica, Cypsela, 6, 89–96, 1987 (in Catalan).

Aubry, T., Dimuccio, L. A., Almeida, M., Neves, M. J., Angelucci, D. E., and Cunha, L.: Palaeoenvironmental forcing during the Middle-Upper Palaeolithic transition in central-western Portugal, Quaternary Res., 75, 66–79, 2011.

Bergadà Zapata, M. M. and Cortés-Sánchez, M.: Secuencia estratigráfica y sedimentaria, in Cueva de Bajondillo (Torremolinos). Secuencia cronocultural y paleoambiental del Cuaternario reciente en la Bahía de Málaga, edited by: Cortés-Sánchez, M., Ser-

vicio de publicaciones, Centro de publicaciones de la Diputación de Málaga, Málaga, 93–138, 2007 (in Spanish).

Bischoff, J. L., Soler, N., Maroto, J., and Julià, R.: Abrupt Mousterian/Aurignacian Boundary at 40 ka bp: accelerator ^{14}C dates from L'Arbreda Cave (Catalunya, Spain), J. Archaeol. Sci., 16, 563–576, 1989.

Bradtmöller, M., Pastoors, A., Weninger, B., and Weniger, G.-C.: The repeated replacement model – rapid climate change and population dynamics in Late Pleistocene Europe, Quatern. Int., 247, 38–49, 2010.

Burjachs, F.: Palinología de los niveles Gravetiense, Solutrense y Postsolutrense de la Cova de L'Arbreda (Serinyà, Girona), Actas de la VII Reunión sobre Cuaternario, Universidad de Santander, AEQUA, Santander, Cantabria, 19–21, 1987 (in Spanish).

Burjachs, F. and Allué, E.: Paleoclimatic evolution during the last glacial cycle at the NE of the Iberian Peninsula, in: Quaternary Climatic Changes and Environmental Crisis in the Mediterranean Region, edited by: Ruiz Zapata, M. B., Dorado, M., Valdeolmillos, A., Gil, M. J., Bardají, T., Bustamante, I., and Martínez, I., Universidad de Alcalá de Henares, Madrid, 191–200, 2003.

Burjachs, F., López-García, J. M., Allué, E., Blain, H.-A., Rivals, F., Bennàsar, M., and Expósito, I.: Palaeocology of Neanderthals during Dansgaard–Oeschger cycles in northeastern Iberia (Abric Romaní): from regional to global scale, Quatern. Int., 247, 26–37, 2012.

Burjachs, F. and Renault-Miskovsky, J.: Paléoenvironment et paleoclimatologie de la Catalogne Durant près de 30000 ans (du Würmien ancien au début de l'Holocène) d'après la palynologie du site l'Arbreda (Gérone, Catalogne), Quaternaire, 3, 75–85, 1992 (in French).

Casellas, S. and Maroto, J.: La faune de l'Auriganien évolué de la grotte de L'Arbreda (Girona, NR Péninsule Ibérique), Résumés des communications, Vème Conférence International ICAZ, Bordeaux, 1986 (in French).

Cortés-Sánchez, M., Morales-Muñiz, A., Simón-Vallejo, M. D., Bergadà-Zapata, M. M., Delgado-Huertas, A., López-Garcia, P., López-Sáez, J. A., Lozano-Francisco, M. C., Riquelme-Cantal, J. A., Roselló,-Izquierdo, E., Sánchez-Marco, A., and Vera-Peláez, J. L.: Palaeoenvironmental and cultural dynamics of the coast of Málaga (Andalusia, Spain) during the Upper Pleistocene and early Holocene, Quaternary Sci. Rev., 27, 2176–2193, 2008.

Courty, M. A. and Vallverdú, J.: The microstratigraphic record of abrupt climate changes in cave sediments in the western Mediterranean, Geoarchaeology, 16, 467–500, 2001.

Courty, M.-A., Goldberg, P., and Macphail, R. I.: Soils and Micromorphology in Archaeology, Cambridge University Press, Cambridge, 344 pp., 1989.

Daura, J., Sanz, M., García, N., Allué, E., Vaquero, M., Fierro, E., Carrión, J. S., López-García, J. M., Blain, H. A., Sánchez-Marco, A., Valls, C., Albert, R. M., Fornós, J. J., Julià, R., Fullola, J. M., and Zilhão, J.: Terrasses de la Riera dels Canyars (Gavà, Barcelona): the landscape of Heinrich Stadial 4 north of the "Ebro frontier" and implications for modern human dispersal into Iberia, Quaternary Sci. Rev., 60, 26–48, 2013.

Delibrias, G., Romain, O., and Le Hasif, G.: Datation par la méthode du carbone 14 du remplissage de la grotte de l'Arbreda, Cypsela, 6, 133–135, 1987 (in French).

D'Errico, F. and Sánchez-Goñi, M. F.: Neanderthal extinction and the millennial scale climatic variability of OIS 3, Quaternary Sci. Rev., 22, 769–788, 2003.

De Vos, W. and Tarvainen, T. (Eds.): Geochemical Altas of Europe, Part 2: Interpretation of Geochemical Maps, Additional Tables, Figures, Maps and Related Publications, ISBN 951-690-960-4 (electronic version), available at: http://www.gtk.fi/publ/foregsatlas/ (last access: 20 December 2012), 2006.

DIN ISO 11277: Soil Quality – Determination of Particle Size Distribution in Mineral Soil Material – Method by Sieving and Sedimentation, German Institute for Standardization, Berlin, 2002.

Eckmeier, E., Egli, M., Schmidt, M., Schlumpf, N., Nötzli, M., Minikus-Stary, N., and Hagedorn, F.: Preservation of fire-derived carbon compounds and sorptive stabilisation promote the accumulation of organic matter in black soils of the Southern Alps, Geoderma, 159, 147–155, 2010.

Ellwood, B. B., Harrold, F. B. Benoist, S. L., Straus, L. G., Gonzalez Morales, M., Petruso, K., Bicho, N. F., Zilhão, J., and Soler, N.: Paleoclimate and Intersite Correlations from Late Pleistocene/Holocene Cave Sites: results from Southern Europe, Geoarchaeology, 16, 433–463, 2001.

Estévez, J.: La fauna del Pleistoceno Peninsular, Ph.D. thesis, Universitat de Barcelona, Spain, 1979 (in Spanish).

Estévez, J.: La fauna de l'Arbreda (sector Alfa) en el conjunct de faunes del Plistocè Superior, Cypsela, 6, 73–87, 1987 (in Catalan).

Evans, M. E. and Heller, F.: Environmental Magnetism, Academic Press, San Diego, London, Burlington, 299 pp., 2003.

Fernández, S., Fuentes, N., Carrión, J. S., González-Sampériz, P., Montoya, A., Gil, G., Vega-Toscano, G., and Riquelme, J. A.: The Holocene and Upper Pleistocene pollen sequence of Carihuela Cave, southern Spain, Geobios, 40, 75–90, 2007.

Geurts, M. A.: Approche palynostratigraphique des dépôts calcaires quaternaires dans la région de Banyoles-Besalú (Catalogne), in: Actas de la IV Reunión del Grupo de trabajo del Cuaternario, edited by: Julià, R., Marqués, M. A., Mir, A., Serrat, D., and Gallart, F., Consejo Superior de Investigaciones Cientificas, Barcelona, 106–116, 1979 (in French).

González-Sampériz, P., Leroy, S., Carrión, J. S., García-Antón, M., Gil-García, M. J., and Figueiral, I.: Steppes, savannahs and botanic gardens during the Pleistocene, Rev. Palaeobot. Palyno., 162, 427–457, 2010.

Höbig, N., Weber, M. E., Kehl, M., Weniger, G.-C., Julià, R., Melles, M., Fülöp, R.-H., Vogel, H., and Reicherter, K.: Lake Banyoles (northeastern Spain): a Last Glacial to Holocene multiproxy study with regard to environmental variability and human occupation, Quatern. Int., 274, 205–218, 2012.

IGME: Geological map, $1:50,000$ sheet Banyoles 295, Instituto Geológic y Minero de España, Madrid, 1987–1989.

ISO 13320-1: Particle Size Analysis – Laser Diffraction Methods, Part 1: General Principles, Annex A: theoretical Background of Laser Diffraction, Geneva, 1999.

Juliá, R.: La conca lacustre de Banyoles-Besalti, Monografies del Centre d'Estudis Comarcals de Banyoles, 188 pp., 1980 (in Catalan).

Kabata-Pendias, A.: Trace Elements in Soils and Plants, 4th Edn., CRC Press, Boca Raton, 520 pp., 2010.

Kabiri, L.: Formations littorals et continentals du Pleistocène Superieur en Languedoc – Roussillon et Catalogne – Étude

géologique des remplissages des Ramandils (Port-la-Nouvelle) et de l'Arbreda (Serinya), Ph.D. thesis, Museum National d'Histoire Naturelle, Institut de Paléontologie Humaine, Paris, 210 pp., 1993 (in French).

Karkanas, P.: Preservation of anthropogenic materials under different geochemical processes: a mineralogical approach: geoarchaeology and Taphonomy, Quatern. Int., 214, 63–69, 2010.

Kehl, M., Burow, C., Hilgers, A., Navazo, M., Pastoors, A., Weniger, G., Wood, R., and Jordá Pardo, J F.: Late Neanderthals at Jarama VI (central Iberia)?, Quaternary Res., 80, 218–234, 2013.

López-García, J. M. and Cuenca-Bescós, G.: Evolution climatique Durant le Pléistocène Supérieur en Catalogne (Nord-est de l'Espagne) d'après l'étude des micromammifères, Quaternaire, 21, 249–258, 2010 (in French).

López-García, J. M., Blain, H.-A., Cuenca-Bescós, G., Ruiz-Zapata, M. B., Dorado-Valiño, M., Gil-García, J. M., Valdeolmillos, A., Ortega, A. I., Carretero, J. M., Arsuaga, J. L., Bermúdez de Castro, J. M., and Carbonell, E.: Palaeoenvironmental and palaeoclimatic reconstruction of the Latest Pleistocene of El Portalón Site, Sierra de Atapuerca, northwestern Spain, Palaeogeogr. Palaeocl., 292, 453–464, 2010.

López-García, J. M., Blain, H.-A., Bennàsar, M., Sanz, M., and Daura, J.: Heinrich event 4 characterized by terrestrial proxies in southwestern Europe, Clim. Past, 9, 1053–1064, doi:10.5194/cp-9-1053-2013, 2013.

Loublier, Y.: Application de l'analyse pollinique a l'ètude du paleoenvironnement du remplissage würmien de la grotte de l'Arbreda (Espagne), Thèse, Université des Sciences et Techniques du Languedoc, Montpellier, 85 pp., 1978 (in French).

Mallol, C., Hernández, C. M., and Machado, J.: The significance of stratigraphic discontinuities in Iberian Middle-to-Upper Palaeolithic transitional sites, Quatern. Int., 275, 4–13, 2012.

Maroto, J.: El pas del paleolític mitjà al paleolític superior a Catalunya i la seva interpretació dins del context geogràfic franco-ibèric, Ph.D. thesis, Universitat de Girona, Girona, 377 pp., 1994 (in Catalan).

Maroto, J., Soler, N., and Fullola, J. M.: Cultural change between Middle and Upper Paleolithic in Catalonia, in: The last Neandertals, the First Anatomically Modern Humans: a Tale about the Human Diversity, edited by: Carbonell, E. and Vaquero, M., Universitat Rovira i Virgili, Tarragona, 219–250, 1996.

Maroto, J., Vaquero, M., Arriazabalaga, A., Baena, J., Carrión, E., Jordá, J. F., Martinón, M., Menéndez, M., Montes, R., and Rosell, J.: Problemática cronológica del final del Paleolítico Medio en el Norte Peninsula, in: Neandertales cantábricos, Estado de la cuestión, Monografías 20 (Museo Nacional y Centro de Investigación de Altamira), edited by: Lasheras Corruchaga, J. A. and Montes Barquín, R., Ministerio de Cultura, Santander, 101–114, 2005 (in Spanish).

Maroto, J., Vaquero, M., Arrizabalaga, Á., Baena, J., Baquedano, E., Jordá, J., Julià, R., Montes, R., van der Plicht, J., Rasines, P., and Wood, R.: Current issues in late Middle Palaeolithic chronology: new assessments from Northern Iberia: the Neanderthal Home: spatial and social behaviours, Quatern. Int., 247, 15–25, 2012.

Martínez, K., García, J., Carbonell, E., Agustí, J., Bahain, J. J., Blain, H. A., Burjachs, F., Cáceres, I., Duval, M., Falguères, C., Gómez, M., and Huguet, R.: A new Lower Pleistocene archaeological site in Europe (Vallparadís, Barcelona, Spain), P. Natl. Acad. Sci. USA, 107, 5762–5767, 2010.

Martínez-Moreno, J., Mora Torcal, R., and de La Torre, I.: The Middle-to-Upper Palaeolithic transition in Cova Gran (Catalunya, Spain) and the extinction of Neanderthals in the Iberian Peninsula, J. Hum. Evol., 58, 211–226, 2010.

Moreno, A., González-Sampériz, P., Morellón, M., Valero-Garcés, B. L., and Fletcher, W. J.: Northern Iberian abrupt climate change dynamics during the last glacial cycle: a view from lacustrine sediments, Quaternary Sci. Rev., 36, 139–153, 2012.

Nesbitt, H. W. and Young, G. M.: Early Proterozoic climates and plate motions inferred from major element chemistry of lutites, Nature, 199, 715–717, 1982.

Onac, B. P., Kearns, J., Cinta Panzaru, S., and Breban, R.: "Variscite (AlPO4 2H2O) from Cioclovina Cave (Sureneau Mountains, Romania): a tale of a missing phosphate", Stud. Univ. Babes-Bol., Geologia, XLIX, 3–14, 2004.

Özer, M., Orhan, M., and Isik, N.: Effect of particle optical properties on size distribution of soils obtained by laser diffraction, Environ. Eng. Geosci., 16, 163–173, 2010.

Pagliai, M. and Stoops, G.: Physical and biological surface crusts and seals, in: Interpretation of Micromorphological Features of Soils and Regoliths, edited by: Stoops, G., Marcelino, V., and Mess, F., Elsevier, Amsterdam, 419–440, 2010.

Pérez-Obiol, R. and Julià, R.: Climatic Change on the Iberian Peninsula recorded in a 30,000-yr pollen record from Lake Banyoles, Quaternary Res., 41, 91–98, 1994.

Pons, A. and Reille, M.: The Holocene and Upper Pleistocene pollen record from Padul (Granada, Spain): a new study, Palaeogeogr. Palaeocl., 66, 243–263, 1988.

Pye, K. and Blott, S.: Particle size analysis of sediments, soils and related particulate materials for forensic purposes using laser granulometry, Forensic Sci. Int., 144, 19–27, 2004.

Ros, M. T.: Anàlisi antracològica de la Cova de l'Arbreda, Cypsela, 6, 67–71, 1987 (in Catalan).

Saladié, P., Vallverdú, J., Bennàsar, M., Cabanes, D., Mancha, E., Menéndez, L., Blain, H.-A., Ollé, A., Mosquera, M., Vilalta, J., Cáceres, I., Expósito, I., Esteban, M., Huguet, R., Rosas, A., Solé, A., López-Polín, L., García, A. B., Martínez, B., Carbonell, E., and Capdevil, R.: Resultats preliminars del nivell 2 del sondeig al Centre de Convencions del barranc de la Boella, Cota Zero, 23, 13–19, 2008 (in Catalan).

Scheinost, A. C. and Schwertmann, U.: Color identification of iron oxides and hydroxysulfates: use and limitations, Soil Sci. Soc. Am. J., 63, 1463–1471, 1999.

Schmidt, I., Bradtmöller, M., Kehl, M., Pastoors, A., Tafelmaier, Y., Weninger, B., and Weniger, G.-C.: Rapid climate change and variability of settlement patterns in Iberia during the Late Pleistocene: temporal and spatial corridors of Homo sapiens sapiens population dynamics during the Late Pleistocene and Early Holocene, Quatern. Int., 274, 179–204, 2012.

Schulze, D. G., Nagel, J. L., van Scoyoc, G. E., Henderson, T. L., Baumgardner, M. F., and Stott, D. E.: Significance of soil organic matter in determining soil colors, in: Soil Color, edited by: Bigham, J. and Ciolkosz, E., American Society of Agronomy, Crop Science Society of America, Soil Science Society of America, Wisconsin, 71–90, 1993.

Sepulchre, P., Ramstein, G., Kageyama, M., Vanhaeren, M., Krinner, G., Sánchez-Goñi, M.-F., and d'Errico, F.: H4 abrupt event

and late Neanderthal presence in Iberia, Earth Planet. Sc. Lett., 258, 283–292, 2007.

Sistiaga, A., Mallol, C., Galván, B., and Summons, R. E.: The Neanderthal Meal: A New Perspective Using Faecal Biomarkers, PLoS ONE, 9, e101045, doi:10.1371/journal.pone.0101045, 2014.

Soler, J., Soler, N., and Maroto, J.: L'Arbreda's archaic Aurignacian dates clarified, Eurasian Prehistory, 5, 45–55, 2008.

Soler, N.: Le Paléolithique des grottes de Serinyà (Gérone, Catalogne, Espagne), in: Les faciès leptolithiques du nord-ouest méditerranéen: milieux naturels et culturels, XXIVe Congrès Préhistorique de France edited by: Sacchi, D., Carcassonne, 26–30 Septembre 1994, Actes du Colloque international, Carcassone (France): société Préhistorique Française, Ministère de la Culture, 195–220, 1999 (in French).

Soler, N. and Maroto, J.: L' estratigrafia de la cova de l'Arbreda (Serinyà, Girona), Cypsela, 6, 53–66, 1987a (in Spanish).

Soler, N. and Maroto, J.: Els Nivells d'ocupació del Paléolitic superior a la Cova de L'Arbreda (Serinyà, Girona), Cypsela, 6, 221–228, 1987b (in Catalan).

Soler, N. and Maroto, J.: Les nouvelles datations de l'Aurignacien dans la Péninsule Ibérique, in: Aurignacien en Europe et au Proche Orient, Actes du XIIe Congrès International des Sciences Préhistoriques et Protohistoriques 2, Bratislava, edited by: Bánesz, L. and Kozlowski, J. K., 162–173, 1993 (in French).

Soler, J., Soler, N., Solés, A., Niell, X., Coromina, N., and Medina, B.: Les excavacions a la cova de l'Arbreda durant les campanyes de 2010 i 2011, XI Onzenes Jornades d'Arqueologia de les comarques de Girona, Girona, 15 i 16 de juny de 2012, Museu d'Arqueologia de Catalunya, Universitat de Girona, Girona, 47–58, 2012 (in Catalan).

Van Vliet Lanoë, B.: Frost action, in: Interpretation of Micromorphological Features of Soils and Regoliths, edited by: Stoops, G., Marcelino, V., and Mess, F., Elsevier, Amsterdam, 81–108, 2010.

Weninger, B. and Jöris, O.: A 14C age calibration curve for the last 60 ka: the Greenland-Hulu U / Th timescale and its impact on understanding the Middle to Upper Paleolithic transition in Western Eurasia, J. Hum. Evol., 55, 772–781, 2008.

Weninger, B., Jöris, O., and Danzeglocke, U.: CalPal-2007. Cologne Radiocarbon Calibration and Palaeoclimate Research Package, www.calpal.de, last access: 21 September 2011, 2008.

Wood, R. E., Barroso, C., Caparros, M., Jorda, J. F., Galvan Santos, B., and Higham, T. F. G.: Radiocarbon dating casts doubt on the late chronology of the Middle to Upper Palaeolithic transition in southern Iberia, P. Natl. Acad. Sci. USA, 110, 2781–2786, 2013.

Wood, R.E., Arrizabalaga, A., Camps, M., Fallon, S., Iriarte-Chiapusso, M., Jones, R., Maroto, J., de la Rasilla, M., Santamaría, D., Soler, J., Soler, N., Villaluenga, A., Higham, TFG: The chronology of the earliest Upper Palaeolithic in northern Iberia: New insights from L'Arbreda, Labeko Koba and La Viña, J. Hum. Evol., 69, 91–109, 2014.

Zilhão, J.: Chronostratigraphy of the Middle to- Upper Paleolithic Transition in the Iberian Peninsula, Pyrenae, 37, 7–84, 2006.

Zilhão J. and d'Errico, F.: The chronology and taphonomy of the earliest Aurignacian and its implications for the understanding of Neandertal extinction, J. World Prehist., 13, 1–68, 1999.

Zilhão J. and d'Errico, F.: La nouvelle bataille aurignacienne, Une révision critique de la chronologie du Châtelperronien et de l'Aurignacien ancien, L'Anthropologie, 104, 17–50, 2000 (in French).

Zilhão J. and d'Errico, F.: The chronology of the Aurignacian and Transitional technocomplexes, Where do we stand? in: The Chronology of the Aurignacian and transitional technocomplexes, Dating stratigraphies, cultural implications, Trabalhos de Arqueología, Instituto Português de Arqueologia, Lisboa, 33, 313–349, 2003.